

**Size distributions of polycyclic aromatic hydrocarbons in urban atmosphere: sorption mechanism and source contributions to respiratory deposition**

5 Y. Lv<sup>1</sup>, X. Li<sup>1</sup>, T. T. Xu<sup>1</sup>, T. T. Cheng<sup>1</sup>, X. Yang<sup>1</sup>, J. M. Chen<sup>1</sup>, Y. Iinuma<sup>2</sup>, and H. Herrmann<sup>2</sup>

<sup>1</sup>Shanghai Key Laboratory of Atmospheric Particle Pollution and Prevention (LAP3),  
Department of Environmental Science & Engineering, Fudan University, Shanghai  
10 200032, China

<sup>2</sup>Leibniz-Institut für Troposphärenforschung (IfT), Permoserstr. 15, D-04318, Leipzig,  
Germany

*Correspondence to:* X. Li (lixiang@fudan.edu.cn)

15 and H. Herrmann (herrmann@tropos.de)

\*Corresponding author. Tel.: +8621-65642298; fax: +8621-65642080

20

## ABSTRACT

In order to better understand the particle size distribution of polycyclic aromatic hydrocarbons (PAHs) and their sources contribution in human respiratory system, size-resolved PAHs had been studied in ambient aerosols at a megacity Shanghai site during a one-year period 2012-2013.

~~Current knowledge on atmospheric particle phase polycyclic aromatic hydrocarbons (PAHs) size distribution remains incomplete. Information is missing on sorption mechanisms and the influence of the PAHs' sources on their transport in human respiratory system. Here we present the studies systematically investigating the modal distribution characteristics of the size-fractioned~~

~~PAHs and calculating the source contribution to adverse health effects through inhalation. Aerosol samples with nine size fractions were collected from Shanghai urban air over one year period 2012-2013. A high correlation coefficient existed between measured and predicted values ( $R^2=0.87$ ), indicated that the data worked very well in current study. Most PAHs were observed on the small particles followed with seasonality differences. When normalized by PAHs across particle diameters, size~~

~~distribution of PAHs exhibited bimodal patterns, with a peak (0.4-2.1  $\mu\text{m}$ ) in fine mode and another peak (3.3-9.0  $\mu\text{m}$ ) in coarse mode, respectively. The results showed the PAHs exhibited a bimodal distribution with one mode peak in the fine particle size~~

~~range (0.4-2.1  $\mu\text{m}$ ) and another mode peak in the coarse particle size range (3.3-9.0  $\mu\text{m}$ ).~~

~~Along with the increasing increase of ring number of PAHs, the intensity of the fine mode peak increased, while coarse mode peak decreased. Plotting of  $\log(\text{PAH}/\text{PM})$  against  $\log(D_p)$  showed that all slope values were above -1 with the increase towards less ring PAHs, suggesting that multiple mechanisms, i.e. (adsorption and~~

~~absorption) controlled the particle size distribution of PAHs. PAHs on particles, but adsorption played a much stronger role for 5- and 6-ring than 3- and 4-ring PAHs. The mode distribution behavior of PAHs showed that fine particles were major carriers for the more ring PAHs. Further calculations using inhaling PAHs data showed (The total~~

~~deposition fluxes of PAHs in respiratory tract were was calculated at  $8.8 \pm 2.0 \text{ ng h}^{-1}$ . Specifically, fine particles contributed 10-40% of PAHs deposition fluxes to the~~

alveolar region, while coarse particles contributed 80–95% of ones to the head region. ~~Estimated~~ The highest lifetime cancer risk (LCR) was estimated at  $1.5 \times 10^{-6}$ . ~~( $1.5 \times 10^{-6}$ )~~ which exceeded the unit risk of  $10^{-6}$ . The LCR values presented in here were mainly influenced by accumulation mode PAHs for people exercised in haze days ( $1.5 \times 10^{-6}$ ) was bigger than the cancer risk guideline value ( $10^{-6}$ ). The largest PAHs contribution for LCR mainly came from the accumulation particles. Based on source apportionment results generated by positive matrix factorization (PMF), it was found that the cancer risk caused in accumulated mode mainly resulted from which came from biomass burning (24%), coal combustion (25%) and vehicular emission (27%). The present study provides us a mechanistic understanding of the particle size distribution of PAHs and their transport in human respiratory system, which can help develop better source control strategies. ~~results contribute to a mechanistic understanding of PAHs size distribution causing adverse health effects and will help develop some source control strategies or policies by relying on respiratory assessment data.~~

**Keywords:** PAHs, size distribution, sorption mechanism, source contributions, respiratory deposition

## 1 Introduction

Atmospheric PAHs are important contaminants in urban air because of their carcinogenic and mutagenic properties (Li et al., 2006; Garrido et al., 2014). They mainly result from incomplete combustion of carbon-containing materials, and can partition between the gas and the particulate phase (Fernández et al., 2002; Hytönen et al., 2009; Shen et al., 2011). This partitioning process strongly depends on particle sizes distribution, PAH compositions species and temperature, and affects the PAHs transport, deposition, degradation processes as well as health impacts. During the partitioning processes Among them, particle size distributions of PAHs play a critical yet poorly understood role. Of particular importance is the role played by high molecular mass PAHs because most of them are carcinogenic and associated with fine aerosol particles (Akyuz and Cabuk, 2009; Wu et al., 2014). Since inhalation deposition depends on

particle sizes, these Fine particles loaded with PAHs can travel deep into the human respiratory system, and cause direct health impact, ~~as inhalation exposure depends on particle sizes~~ (Kawanaka et al., 2009; K. Zhang et al., 2012b). Current knowledge on PAHs size distribution remains incomplete. Information is missing on partitioning mechanisms and health affect of PAHs.~~Information is missing on sorption mechanisms and the influence of the PAHs' sources on their transport in human respiratory system.~~

To address these concerns, further studies are necessary and significant.

Over the past decade, numerous measurements on PAHs size distribution have been repeatedly carried out in various areas around the world such as Seoul (Korea) (Lee et al., 2008), Saitama, Okinawa (Japan) (Kawanaka et al., 2004; Wang et al., 2009), Mumbai, Delhi (India) (Venkataraman et al., 1999; Gupta et al., 2011), Barcelona (Spain) (Mesquita et al., 2014), Dresden (Germany) (Gnauk et al., 2011), Birmingham (England) (Delgado-Saborit et al., 2013), Lisbon (Portugal) (Oliveira et al., 2011), Algiers (Algeria) (Ladji et al., 2014), Beauharnois (Canada) (Sanderson and Farant, 2005), Los Angeles, Massachusetts, Chicago, Claremont (USA) (Venkataraman and Friedlander, 1994; Allen et al., 1996; Offenberg and Baker, 1999; Miguel et al., 2004), Tianjing, Beijing, Guangzhou (China) (Wu et al., 2006; Zhou et al., 2008; Yu and Yu, 2012). These studies, conducted in various countries and cities, showed that most PAHs existed on small particles and had a similar modal distribution for isomers. PAHs size distribution can vary with their releasing sources and ~~change through~~ particle aging processes ~~in the atmosphere~~ (Venkataraman et al., 1994). In order to illustrate the partitioning mechanism of PAHs among-between particles, Venkataraman et al. (1999) developed the equilibrium adsorption and absorption theory, which explained the predominance of PAHs in nuclei and accumulation mode particles, respectively, but failed to explain ~~the preferential accumulation of less ring PAHs compared to more-ring PAHs~~ in coarse mode. Allen et al. (1996) proposed that mass transfer by vaporization and condensation ~~helps~~ helped estimate the particle size distribution of PAHs. However, this theory ~~does~~ did not account for particle deposition and ~~its~~ their ~~impact~~ influence on residence time. Therefore, the mechanisms that govern PAHs

distribution in different size particles ~~distributing in a range of particle sizes~~ are not still disputable and require further clarification. The fine particles discussed here can travel deep into the human respiratory system and, for the smallest particles, potentially enter the bloodstream, thus exposing the ~~person~~ people to both particles and the particle-bound compounds (Geiser et al., 2005). To solve these problems, the first thing we should figure out the releasing source of size-specific PAHs as well as clarify their transport characteristics in human respiratory system (Chen and Liao, 2006; Sheesley et al., 2009). ~~on size-specific particles. However, current studies associated with source apportionment of atmospheric PAHs often do not account for size distribution and their impact on mechanism, deposition and transport in human respiratory system (Chen and Liao, 2006; Sheesley et al., 2009). Understanding PAHs sources attribution on size-specific particles is thus crucial to better describe their atmospheric fate and understand and reduce human exposure.~~

The present ~~paper~~ study aims to ~~contribute to the knowledge base by conducting~~ conduct ~~an~~ ambient measurements on ~~aerosol~~ particle size distributions of PAHs associated with inhalation exposure at ~~in~~ a megacity Shanghai site during a one-year period 2012-2013. ~~over a one year period. We specifically aim to determine whether there are relationships in the PAHs releasing sources and the involved mechanism associated with adsorption, absorption and inhalation exposure—the main~~ The specific objectives ~~of our research~~ are as follows: (i) to investigate particle size distributions of ~~atmospheric~~ PAHs; (ii) to elaborate the ~~atmospheric~~ mechanisms and process controlling PAHs distribution among the different size particles ~~among size-resolved particles~~; and (iii) ~~to identify local sources for PAHs on size-specific particles, and (iv) to estimate the~~ inhalation exposure and PAHs' source contribution. ~~to human respiratory tract through inhalation exposure.~~

## 2 Experimental and methods

### 2.1 Chemicals

All solvents were HPLC grade and bought from Tedia Company Inc, USA. Standard mixtures of PAHs were purchased from Sigma-Aldrich, Shanghai, China. The 16 EPA

priority PAHs were investigated, i.e. naphthalene (NAP, 2-ring), acenaphthylene (ANY, 3-ring), acenaphthene (ANA, 3-ring), fluorene (FLU, 3-ring), phenanthrene (PHE, 3-ring), anthracene (ANT, 3-ring), fluoranthene (FLT, 4-ring), pyrene (PYR, 4-ring), benz[a]anthracene (BaA, 4-ring), chrysene (CHR, 4-ring), benzo[b]fluoranthene (BbF, 5-ring), benzo[k]fluoranthene (BkF, 5-ring), benzo[a]pyrene (BaP, 5-ring), dibenz[a,h]anthracene (DBahA, 5-ring), indeno[1,2,3-cd]pyrene (IPY, 6-ring), and benzo[ghi]perylene (BghiP, 6-ring). For the purpose of ease of discussion, we divided these PAHs into four groups, i.e. 3- to 6- ring PAHs based on their volatility and aromatic ring numbers (Allen et al., 1996; Duan et al., 2005, 2007).

## 10 2.2 Sampling site

The measurements took place on the rooftop (20 m above the ground) of No.4 teaching building at Fudan University campus (121.50E, 31.30N), approximately 5 km northeast of downtown Shanghai city (elevation about 4 m a.s.l.). ~~This~~There is a Fudan super monitoring station for atmospheric chemistry running all year round. More information on this site can be found in previous studies (X. Li, 2011; P. F. Li et al., 2011), and hence only a brief introduction is given. The site is located in a mixed-used neighborhood including many schools, supermarkets and residences. The site is also in close proximity to two major streets, i.e., Handan Road (about 200 m south) and Guoding Road (about 300 m east); ~~which is the main corridor leading to Xiangyin Tunnel (Huangpu river) and Yangpu bridge.~~ There is always heavy traffic in this area due to the local and cross-border traffics. The main releasing ~~sources of local air pollution~~ at this site include industries emission, household heating, road transport and biomass burning.

## 20 2.3 Sample collection and pretreatment

25 An Anderson 8-stage air sampler (Tisch Environmental Inc.~~Thermo-Electron Corporation~~, USA) was used to collect aerosol samples with different size ranges, i.e. 10.0 (inlet)-9.0, 9.0-5.8, 5.8-4.7, 4.7-3.3, 3.3-2.1, 2.1-1.1, 1.1-0.7, 0.7-0.4 and <0.4  $\mu\text{m}$  (backup filter). ~~Based on the need of this research, the fractions were divided into~~

~~three modes: aitken ( $dp < 0.4 \mu\text{m}$ ), accumulation ( $0.4 < dp < 2.1 \mu\text{m}$ ) and coarse ( $dp > 2.1 \mu\text{m}$ ) mode.~~ The flow rate of the sampler was controlled at  $28.3 \text{ L min}^{-1}$ . The average collecting time for each batch of samples was 120 h, and the air volume that passed through the sampler was of  $203.8 \text{ m}^3$ . The sampling campaign was conducted during the period 12, 2012 - 12, 2013. A total of 189 size-segregated particle samples ~~were~~ was obtained including their corresponding sampling information and meteorological conditions.

Quartz fiber membranes (Whatman QMA,  $\varnothing$  81 mm) were used to collect aerosol particle samples. Before using, the membranes were baked at  $450 \text{ }^\circ\text{C}$  for 4 h, equilibrated at  $20 \text{ }^\circ\text{C}$  and 40% relative humidity for 24 h, and then weighed. After sampling, the membranes were equilibrated at  $20 \text{ }^\circ\text{C}$  in a desiccator for 24 h and weighed again using the same procedure. Then, the membranes were stored in freezers at  $-20 \text{ }^\circ\text{C}$  until they were extracted. Extraction was performed as soon as possible to ~~before some~~ ensure minimal loss of volatile less ring-PAH congeners/species ~~volatilized.~~ The procedure applying for PAHs pretreatment was Soxhlet extraction. Briefly, the filter samples were put in a Soxhlet apparatus and extracted in a refluxing dichloromethane/hexane (1:1, v/v) for 36 h. The temperature was controlled at  $69 \text{ }^\circ\text{C}$ . After the extraction was completed, the contents were filtered by a  $0.45 \mu\text{m}$  PTFE membrane to remove insoluble particles, and then concentrated to exactly 2 mL by rotary evaporator and under gentle nitrogen stream. The final extracts were stored in the refrigerator for further quantitative and qualitative analysis. The detailed pretreatment procedure could be found elsewhere (Mai et al., 2003).

## 2.4 Analytical procedure

All samples were quantified for 16 PAHs by an Agilent 7890A Series GC coupled to an Agilent 7000B Triple Quadrupole MS (GC/MS/MS, Agilent Technologies Inc., USA) operated in EI mode. The analysis was performed using the Multiple Reaction Monitoring (MRM) procedure. The separation was achieved with a HP-5MS capillary column ( $30 \text{ m} \times 0.25 \text{ mm i.d.} \times 0.25 \mu\text{m}$ ). The GC oven temperature was programmed from  $70 \text{ }^\circ\text{C}$  (hold for 2 min) to  $280 \text{ }^\circ\text{C}$  at  $15 \text{ }^\circ\text{C min}^{-1}$ , and finally  $310 \text{ }^\circ\text{C}$  at  $5 \text{ }^\circ\text{C min}^{-1}$

with a hold of 1 min. The total program time was 23 min. The temperatures of the injector, ion source and transfer line were controlled at 310, 300 and 310 °C, respectively. Analyses were carried out ~~in the~~ at a constant flow mode. Ultra high purity Helium (99.999%) was applied as carrier gas with the flow rate of 1.2 mL min<sup>-1</sup>.

5 Nitrogen was used as collision gas.

Matrix-matched calibration curves (5 to 1000 ng mL<sup>-1</sup>) were obtained for all compounds on the GC/MS/MS instrument, by plotting the compound concentration vs. the peak area and determining the R<sup>2</sup> using weighted linear regression (1/x) with the quantitative analysis software for GC/MS/MS. Limits of detection (LODs) and limits of quantification (LOQs) were measured based on signal to noise ratio at about 3 and 10, respectively. The average blank value ~~is~~ was subtracted from each signal being above the LOD. Recovery tests were used to estimate possible losses of PAHs during the extraction process. The blank filters were spiked with the standard mixture and gone through the same procedures for analysis. The results (n=3) showed that the mean recoveries ranged 70% to 100% for all PAHs. All concentrations reported were corrected by their respective recovery percentage.

## 2.5 Statistical analysis

Statistical analysis was carried out using partial least-squares regression (PLS) procedure in the SIMCA-P software (Version 11.5, Umetrics Inc., Umeå Sweden). The size-segregated particles and corresponding PAHs contents ~~are~~ were respectively used as Y-variables and X-variables in PLS model. All variables were centred and scaled to unit variance before the analysis. Thereby all variables contributed with equal weight to the model. An important parameter in PLS analysis is the cross-validation correlation coefficient ( $Q^2$ ), which is calculated from predicted residual sum of squares and can give an evaluation of the model's predictive ability in SIMCA (Lindgren et al., 1995). A large  $Q^2$  value (>0.5) means that the PLS model has a predictivity better than chance. In addition, the observed ~~vs.~~ versus predicted plot ~~to~~ can give a more direct displays for the values of the selected response. The correlation coefficient (R<sup>2</sup>) between observed and predicted can be utilized for the evaluation of the goodness of model fit. Generally,



R<sup>2</sup> value ~~greater~~ higher than 0.8 indicates PLS model ~~constructed in software~~ fits well with the data.

## 2.6 PMF source apportionment

Source apportionment of the size-~~segregated~~ resolved PAHs was performed using Positive Matrices Factorization (PMF). In the following, PMF will be shortly outlined (Larsen and Baker, 2003; Ma et al., 2010b). By analyzing measured concentrations at receptor sites, the method can identify a set of factors which can be taken to represent major emission sources (Paatero and Tapper, 1994). PMF models are expressed as follows:

$$x_{ij} = \sum_{k=1}^p g_{ik} f_{kj} + e_{ij} \quad (\text{Eq. 1})$$

Where  $X$  is a data matrix of  $i$  by  $j$  dimension, in which  $i$  is the number of the size-segregated particle samples and  $j$  is the number of the measured PAH species.  $f_{kj}$  is the concentration of the  $j$ th PAH species in the emissions from the  $k$ th source;  $g_{ik}$  is the contribution of the  $k$ th source to  $i$ th particle sample.  $e_{ij}$  is the portion of the measured concentration that cannot be explained by the model.

By incorporating an uncertainty for each observation  $u_{ij}$ , the PMF solution can minimize the objective function  $Q$  (Eq. 2),

$$Q = \sum_{i=1}^n \sum_{j=1}^m \left[ \frac{x_{ij} - \sum_{k=1}^p g_{ik} f_{kj}}{u_{ij}} \right]^2 \quad (\text{Eq. 2})$$

The PMF model requires data on measured PAH concentrations for all samples, together with information on the associated uncertainties. The confidence of results can be maintained by adjusting the data uncertainties. This allows us to lower down the importance of these data through the least squares fit. The work presented here is the US EPA PMF version 3.0. Please find more information about these on US EPA website (<http://www2.epa.gov/air-research/positive-matrix-factorization-model-environmental-data-analyses>). (~~<http://www.epa.gov/heads/research/pmf.html>~~)

## 2.7. Human respiratory risk assessment

In order to evaluate the influence of the size-resolved PAHs on human respiratory potential~~the human respiratory potential of the size-segregated PAHs~~, we adopted an International Commission on Radiological Protection (ICRP) model (ICRP, 1994) for these. Based on inhaled particles sizes, the respiratory tract ~~is~~ was divided into three main deposition regions: head airway (HA), tracheobronchial (TB) and alveolar region (AR)~~regions: head, tracheobronchial, and alveolar region~~. The PAH concentrations were loaded into the ICRP model to calculate the deposition efficiency and flux of inhaled PAHs.

Lifetime cancer risk (LCR) were applied to assess the cancer risk associated with exposure to the size-~~segregated~~ resolved PAHs through inhalation of ambient particles (Kawanaka et al., 2009; K. Zhang et al., 2012b). The LCR ~~can then be~~ were calculated by the formula (US EPA, 1989):

$$LCR = EI \times ED \times CSF / (AT \times BW) \quad (\text{Eq. 3})$$

where EI ~~is~~ was the estimated inhalation rate ( $\text{mg d}^{-1}$ ) which ~~is~~ was calculated by deposition fluxes ( $\text{mg h}^{-1}$ ) and daily exposure time ( $12 \text{ h d}^{-1}$ ), ED ~~is~~ was the exposure duration for an adult (30 years), CSF ~~is~~ was the inhalation cancer slope factor ( $(\text{mg kg}^{-1} \text{ d}^{-1})^{-1}$ ), BW ~~is~~ was the body weight ( $\sim 60 \text{ kg}$ ); and AT ~~is~~ was the average lifetime for carcinogens (assuming 70 years for adults). LCR for exposure to PAHs in this paper was based on the sum of BaP equivalent concentration ( $\text{BaP}_{\text{eq}}$ ) which calculated by multiplying each concentration by its individual toxic equivalency factor (TEF) (Nisbet and Lagoy, 1992). As suggested by the OEHHA, a value of 3.9 of BaP was usually applied as a recommended value for the calculation of CSF in LCR formula (Liu et al., 2007).

### 3. Results and discussion

#### 3.1 Occurrence and Size Distribution of PAHs

~~Figure~~ Fig. 1 presents the time variation~~trend~~ of the total PAHs, size-segregated particles, visibility and relative humidity (RH) during the sampling period. Results show high PAHs episodes coincide with high PM levels, along with the low RH and low visibility.

Average total PAH concentrations adsorbed on particles range from 41.6 to 66.6 ng m<sup>-3</sup> (average: 48.7 ng m<sup>-3</sup>). The concentration of total particles during the observation period varies from 54.8 to 209.6 μg m<sup>-3</sup> (average: 122.8 μg m<sup>-3</sup>). Among them, the daily PM<sub>2.5</sub> concentration is 61.8 μg m<sup>-3</sup>, which is obviously higher than the annual (daily) national air quality standard of 10 (25) μg m<sup>-3</sup> set by the World Health Organization (WHO 2005). Most particles masses is found in the accumulation mode size ranges (0.4-2.1 μm). Fine particles are typically higher than coarse particles in Shanghai air. This finding is consistent with previous research on particle size distribution in Shanghai (Wang et al., 2014). The PM<sub>2.5</sub>/PM<sub>10</sub> ratio of 50(±8)% (~~50±8%~~) suggests that the anthropogenic component of particle matter as represented by the PM<sub>1</sub> fraction is significant in the studied area (Theodosi et al., 2011).

For the investigation of seasonal trends, the PAHs data is divided into 4-four seasonal groups, i.e. spring (March to May), summer (June to August), autumn (September to November) and winter (December to February). ~~There is a distinct seasonal cycle for total PAHs with higher values in winter than in summer (Fig. 2) corresponding to temperature differences first of all. The amplitude of the cycles depends on particle size, for example, PAHs concentrations are generally higher in the fine particles ( $d_p < 2.1 \mu\text{m}$ ) than in the coarse particles ( $d_p > 2.1 \mu\text{m}$ ). This fact indicates that total PAHs are mainly adsorbed onto small particles due to their extremely large available surface.~~ Fig. 2 shows seasonal variation of PAHs average concentration in aerosol particles. Results indicate that the mean concentration of particle-bound PAHs undergo distinct seasonal variation, i.e., the highest levels in cooler seasons, while lowest or below detection limit during warmer seasons. The most abundant PAH species in winter are 5- and 4-ring PAHs (16 and 13 ng m<sup>-3</sup>), followed by 6- and 3-PAHs (7.5 and 6.5 ng m<sup>-3</sup>). Given these data, it can be pointed out that the season variation and particle size influence the concentration of PAHs. Shanghai is situated in the subtropics along the east coast of China continent. The seasonal variation of weather in Shanghai is closely related to and controlled by the northern subtropical monsoon system. In winter, the popular northwest wind can drive the air pollutants from the north China

mainland to Shanghai, while in summer, the popular southeast wind can bring clean oceanic air mass from the Pacific Ocean to Shanghai. In cold seasons (winter and autumn), elevated winter- and fall-time PAHs concentrations, particularly at urban sites, are most likely due to the higher level of fresh emissions from primary sources (such as wood smoke and vehicular emissions). Moreover, cold-ignition of gasoline-powered vehicles during cold seasons may lead to an increase in the level of high molecular weight PAHs such as 4- to 6-PAHs (Arhami et al., 2010). The atmospheric conditions in winter such as low temperatures, low intensity of solar radiation and decreased PAHs photo-degradation also favor the condensation/adsorption of PAHs on suspended particles that presented in urban air. On the other hand, in warm seasons (summer and spring), the concentrations of PAHs are reduced, possibly due to the high temperatures, higher mixed layer height, and heavy rainfall that may effectively remove particle-bound PAHs from the atmosphere. Additionally, high temperature and solar radiation favor the photo-chemical oxidation of PAHs. This seasonal pattern has been reported in many urban atmospheres. ~~Seasonal differences may be related to ambient temperature and the different volatilities of PAH compounds. This seasonal variation is similar to the findings in other places for atmospheric PAHs (Teixeira et al. 2012; van Drooge and Ballesta, 2009; Ma et al., 2010a). The different distribution patterns of PAHs in fine and coarse particles may be attributed to different emission mechanisms of PAHs in urban areas.~~ More details will be included in the following detailed mode discussion and source attribution of PAHs. ~~discussion about mode analysis and source attribution associated with size distribution.~~

~~Some empirical evidence suggests that PAHs with similar molecular weights or ring numbers maybe have similar aerosol particle size distributions (Allen et al., 1996; Duan et al., 2005, 2007). Based on their volatility and aromatic ring numbers, 16 PAHs are divided into four groups, i.e. 3- to 6- ring PAHs. To better describe PAHs distributions, the particle fractions are divided into three modes: Aitken ( $dp < 0.4 \mu\text{m}$ ), accumulation ( $0.4 < dp < 2.1 \mu\text{m}$ ) and coarse ( $dp > 2.1 \mu\text{m}$ ) mode. The Aitken and accumulation modes together constitute “fine” particles. We~~ the commonly used way isto-plot a log-

log chart, i.e.,  $dC/d\log D_p$  is plotted against  $D_p$  (Particle diameter) on the log scale, in which where  $dC$  is the PAHs concentrations in each particle size bin and  $d\log D_p$  is the size width of each impactor channel (Kawanaka et al., 2004; Venkataraman and Friedlander, 1994; Venkataraman et al., 1999). Figure Fig. 3 clearly demonstrates shows that the size distribution most of PAHs have a bimodal particle-size distribution which contains one mode peak in accumulation size range (0.4-2.1  $\mu\text{m}$ ) and another mode peak in coarse size range (3.3-9.0  $\mu\text{m}$ ), exhibited bimodal patterns, with a peak (0.4-2.1  $\mu\text{m}$ ) in fine mode and another peak (3.3-9.0  $\mu\text{m}$ ) in coarse mode. The As the numbers of PAHs' aromatic ring increases, the intensities of two peaks intensities vary a lot towards larger PAHs, i.e., the accumulation mode peak increases, while coarse mode peak decreases the peak in accumulation mode becomes more predominant, while another one in coarse mode becomes weaker and even disappears for at 5- and 6-ring PAHs. This is due to the fact that because less volatile PAH species compounds preferentially condense on fine particles and more volatile ones PAH species are inhibited on smaller particles because of the Kelvin effect (Hien et al., 2007; Keshtkar and Ashbaugh, 2007). This kind of mode distribution mode that appears in Shanghai is similar to those found in Mumbai, India (Venkataraman et al., 1999), but different with those not same in Boston, MA (Allen et al., 1996). From the results of PAHs distribution, one we can also obtain an important implication for of health hazards via inhalation exposure. Since the majority of larger high molecular weigh PAHs has mutagenic and/or carcinogenic properties and almost exclusively exists on fine particles, they which can travel deep into the human respiratory system and hence can cause a serious health risk through exposing a person to both particles and the loaded carcinogenic PAHs (Kameda et al., 2005).

### 3.2 Atmospheric Processing and Partitioning Mechanisms

Previous studies on atmospheric process of PAHs mainly focus on gas/particle partitioning (R. Zhang et al., 2012; McWhinney et al., 2013), but few studies focus on are associated with the aerosol particle size distribution of PAHs. For these, we use the size-resolved PAHs data to To further understand the significance of size

dependency during the PAHs atmospheric processing, size fractionated PAHs data acquired in the present study are used to assess the PAHs partitioning process between among different size particles sizes.

Empirical evidences suggest mass ratios of PAH to particulate matter (PAH/PM) can provide some valuable implications for PAHs atmospheric process. When PAH compounds ~~that~~ and particles that produced from incomplete combustion of organic material are released into the air, ~~from incomplete combustion of organic material are mainly associated with size segregated aerosol particles through adsorption and absorption. The size-resolved PAHs would~~ they should be involved in the particle aging process of aerosol. During this process, atmospheric ~~because some~~ PAHs ~~could~~ could be photo-oxidized to form SOA ~~secondary organic aerosol~~ (Secondary organic aerosol SOA), and others might adsorb or absorb on preexisting particles via either self-nucleation or gas/particle partitioning. This would lead to the increase of atmospheric fine particulate matter ~~increasing organic fine particulate matter through either self-nucleation or gas particle partitioning~~ (Kavouras et al., 1999; Kamens et al., 1999; Yu et al., 1999; Kamens and Jaoui, 2001; Chan et al., 2009). That is to say that the aging process can decrease the value of total-PAH/PM ~~That means that the aging process will reduce the value of PAH/PM~~ (Duan et al., 2005; Bi et al., 2005). Figure ~~Fig.~~ 4 shows the variation of total PAHs/PM values ~~by size~~ across particle sizes ~~all the samples demonstrating that values for the ratio PAH/PM range between 0.01 and 0.1 depending on PAH species characteristics~~. In general, PAH/PM ratios decrease gradually ~~towards particles~~ with the increase of particle ~~bigger~~ size. This indicates that the different values of PAH/PM across particle size can be the result of different aging process. However, it should be noted that 5 and 6 ring PAH/PM ratios showed a little increasing fluctuation during the size range 2.1–5.8  $\mu\text{m}$ . The reasons for this phenomenon are unclear but may be related to long repartitioning process of low volatile 5 and 6 ring PAHs in coarse particles due to the lower vapour pressures (Bi et al., 2005), or mass of PM in this size range decreased by dry and wet deposition or forming larger particles through coagulation. The isomer ratio of a more reactive PAH to a stable PAH, such as

BaA/Chr and BaP/BeP, can be employed to illustrate the PAHs atmospheric fate (Ding et al., 2007). In order to further verify the particle aging process, we use BaA/CHR as another indicator of particle aging. BaA is expected to be degraded more easier than their isomers during transportation period because of their higher reactivity. Using the ratios of a more reactive PAH compound to a less reactive one, such as BaA/CHR, An/Phe and BaP/Bep, a higher ratio indicates relatively little photochemical processing of the air mass. On the other hand, a lower ratio is reflective of more aged PAHs. Therefore, it can be used to illustrate whether the air masses collected are fresh or aged (Ding et al., 2007). Fig. 4 shows the decrease of BaA/CHR with the increase of particle sizes, which is the same trend with PAH/PM. Generally, relatively higher ratios occur in small particle size ranges, and lower ratios exist in large particle size ranges, suggesting smaller particles sampled at urban sites are relatively fresh, while bigger particles are relatively aged. Because particulate phase PAHs are susceptible to photo-degradation, the decrease of BaA/CHR with the increase of particle sizes shows that photo-degradation play an important role in particle aging process, especially for the relatively larger urban aerosol particles. During this transport process, BaA and BaP are expected to degrade more easily than their isomers, so the ratios will be modified by their strong reactivity. Naturally, the values would degrade over transport time (Duan et al., 2005). Figure 5 reveals the variations of BaA/Chr CHR by size across all the samples. Apart from a few particular values during the size range 5.8-10.0  $\mu\text{m}$ , the majority declines with the increase of particle size. This trend is approximately in accord with the changes of total PAH/PM across all samples. This indicates that PAH species are indeed involved in the processes of changing particle size distribution or aerosol aging, and can provide some information about the aging degree to a certain extent. Nevertheless, aerosol aging estimated by size-fractionated PAHs in the present study It should be noted that the explanation of particle aging in the present study still meets remain some uncertainties because of the scarcity of “aging time scale” data, some correlative variabilities such as particle increase velocities and meteorological conditions. Again, only size distribution of PAHs during the atmospheric process are estimated in the present study, therefore further studies (e.g.,

particle and PAH formation theoretical models and chamber simulation experiment (corresponding influencing mechanisms) are needed to provide more insights into the particle aging associated with PAHs. Although the present study ~~does~~ results do not look directly at the partitioning process, it has taken advantage of the size-fractionated resolved PAHs data to examine the governing mechanisms for aerosol particle size distribution.

Currently, the reliable mechanisms for controlling PAHs distribution in-between size-resolved different size particles include adsorption to nucleus particles, adsorption and absorption to accumulation particles, and multilayer adsorption on coarse particles (Venkataraman et al., 1999). Adsorption and absorption depend respectively on available particle surface area and organic mass. If PAHs are firstly associated with the particle surface, the PAH/PM mass ratio will show a  $1/D_p$  dependence (assuming particles are spherical), and then will generate a straight line of slope -1 on a log vs. log axis (Venkataraman et al., 2002). Fig. 5 shows that all slope values from the plots Plotting of  $\log(\text{PAH/PM})$  against  $\log(D_p)$  ~~showed that all slope values were~~ are above -1 ~~with the decrease towards to the more ring PAHs (Fig.6)~~, suggesting that multiple mechanisms, i.e. adsorption and absorption controlled the PAHs' distribution among ~~on~~ different size particles. Moreover, the slope values decrease with the increase of ring number of PAHs, which means ~~but~~ adsorption played a much stronger role ~~for~~ in the distribution process of 5- and 6-ring than 3- and 4-ring PAHs. The reason is due to ~~This might be caused by~~ the relatively lower volatility of 5- and 6-ring PAHs which make ~~compared to smaller ones letting the~~ more compounds adjust to multiple adsorptive equilibrium more slowly. Moreover, chemical affinities maybe also play an important role in adsorption process. Most 5- and 6 ~~more~~-ring PAHs have strong hydrophobicity and tend to affiliate with small particles because they can provide large surface areas (Venkataraman et al., 1999). Such an explanation, however, can not adequately account for ~~the~~ PAHs' equilibrium mechanisms observed in the present study. Perhaps in fact 5- and 6 ~~more~~-ring PAHs do not attain equilibrium due to the slow mass transfer, but they reach a steady state between the gaseous and particulate phases (Yu and Yu, 2012).



### 3.3 Statistical analysis

In an attempt to understand how ~~the alterations in~~ particle size ~~may lead to variations~~ ~~in~~ affect PAH species, we built a statistical model using PLS regression based on PAHs concentration and particle size data ~~all PAHs data~~. After calculating, five components are adopted because they can give the most stable results and easily interpretable factors. The number of components in PLS is also consistent with the results of the followed ~~PMF results~~, as discussed in the next section. By plotting the observed (measured) ~~values~~ particle sizes versus the predicted ~~values~~ particle sizes, ~~for the particle sizes included in the models~~, we ~~got~~ obtain a goodness of fit with  $R^2 = 0.87$ , a goodness of prediction with  $Q^2 = 0.80$ , and a goodness of root mean square error (RMSE) with a value of 0.87. ~~the root mean square error of the fit for observations in with a RMSEE value of 0.87. Figure 7~~ Fig. 6 shows the observed vs. predicted plot ~~for~~ from the model. The plot performs well in predicting the size-resolved PAHs over the size range between 0.4 ~~µm~~ and 10 µm. There is no systematic underestimation (or overestimation) and most points fall close to 45 degree line. The results achieve the desired separation without overlap among nine ~~eight~~ particle size ranges. ~~Most variations of size-resolved PAHs, i.e., up to 80% can be predicted by the parameterization.~~ The model can explain 91% of X, 87% of Y and predict 80% of Y. These predictions are not de novo predictions, since all the data are part of the observed set. Nevertheless, these predicted results do validate the model effectiveness and the measured data reliability.

Similarities between PAHs profiles at the two adjacent sizes can be further identified by coefficient of divergence (CD), which is a self-normalizing parameter used to evaluate the divergence degree of two sets of data (Kong et al., 2012). CD is determined as follows:

$$CD_{jk} = \sqrt{\frac{1}{p} \sum_{i=1}^p \left( \frac{x_{ij} - x_{ik}}{x_{ij} + x_{ik}} \right)^2} \quad (\text{Eq. 4})$$

Where j and k stand for the two adjacent particles fractions, p ~~was~~ is the number of investigated PAHs, and  $x_{ij}$  and  $x_{ik}$  represented the concentrations of PAHs species i for

size j and k (Kong et al., 2011). CD is ranging from 0 to 1. A low CD value (<0.2) indicates a high level of homogeneity in PAHs distribution between two adjacent sizes, while CD values larger than 0.2 indicate heterogeneous PAHs spatial distribution (Wilson et al., 2005). ~~Figure 8~~Fig. 7 shows the PAHs' CD diagrams that are characterized by color block. For the comparison between the adjacent sizes, ~~the most~~ CD<sub>jk</sub> values were are all less than 0.2 except CD<sub>0.4, 0.4-0.7</sub> (0.26) and CD<sub>1.1-2.1, 2.1-3.3</sub> (0.31), indicating that PAHs among PM<sub>0.4</sub>, PM<sub>0.4-2.1</sub> and PM<sub>2.1-10</sub> show a high spatial heterogeneity ~~in the two adjacent sizes fractions show a high spatial homogeneity of the in~~ source factor contributions.

### 10 **3.4 Emission Source of Size-~~Fractionated~~ resolved PAHs**

The different ~~distribution patterns of~~ PAHs distribution in between fine and coarse particles may be attributed to different emission ~~sources mechanisms of~~ PAHs. By applying the PMF model, The optimal five main ~~source~~ factors have been chosen ~~in this study~~ after comparing three or four main factors. Five identified sources ~~for the~~ PAHs are respectively associated with vehicular emission, biomass burning, coal combustion, petroleum residue and air-surface exchange. ~~Figure 9~~Fig. 8 shows the profiles for all factors. Factor 1 presents a profile with high factor loadings for 5- and 6-ring PAHs, i.e. B(b+k)F, BaP, IPY, DBahA and BghiP. These high molecular weight PAHs are reported as dominant in vehicle emissions (Bostrom et al., 2002; Ravindra et al., 2008). BbF and BkF are attributed to diesel motor vehicle emissions, while BaP and BaA are attributed to gasoline and diesel markers (Harrison et al., 1996; Sofowote et al., 2008). Thus, this factor is named as vehicular emissions without distinguishing between diesel and gasoline releasing. Factor 2 is dominated by high loadings of PHE, Flu and BbF and moderate loadings of ~~Chr~~CHR, BkF, BaA, IP and BghiP. This factor profile mainly ~~came~~ come from biomass burning that has been described in the previous study (Poulain et al., 2011). As the occurrence of biomass burning in Shanghai city is normally low, this source is most likely from ~~long~~ long-range transport, rather than from local ~~releasing~~ emission. Factor 3 is characterized by B(b+k)F, CHR, BaA and BghiP. These compounds have been reported by different authors as coal combustion source

markers (Yang et al., 2002; Lin et al., 2011). Although in Shanghai, natural gas is one of the main fuels used for domestic heating, there are still central heating systems using coal and petrol-derived fuels. Moreover, the influence of power plant, ~~soaking~~, steel and iron industries using coal as fuel ~~could~~-may be also reflected on this factor. Factor 4 is  
5 mainly defined by 4- and 5-ring PAHs. High levels of these compounds, especially for PHE are associated with crude oil or refined petroleum emission and their degradation products (Zakaria et al., 2002). So this factor is likely to represent petroleum residue, or the derivatives from oil spill, the leakage from vehicles, and the discharge from municipal and industrial wastewater, etc. Factor 5 is more influenced by 2- and 3-ring  
10 PAHs. These ~~less-ring~~ PAHs are favored in air-surface exchange (Gigliotti et al., 2002). The “exchange” here means that the aged PAHs are probably released into the atmosphere again from contaminated soil or wastewater, and then adsorbed later by the particles. Moreover, they are also arrived at~~transported to~~ here through ~~long~~-long-ranges transport and finally deposit on particle surfaces. Thus, factor 5 is ascribed to air-surface  
15 exchange.

Fig. 9 summarizes the results of PAHs’ source apportionment associated with factor contributions.~~Based on the source apportionment results, the contributions of each factor are summarized in Fig. 10.~~ As expected, the results are quite different for the different~~between~~ particle sizes. Coal combustion and biomass burning respectively accounted for 29% and 29% of ~~total PAHs in~~ accumulation mode PAHs aerosols,  
20 ~~whereas they are~~ as well as 12% and 13% in coarse mode PAHs aerosols. Their contribution for particulate PAHs significantly decreases with the increase~~ing of~~ of particle size ~~due to~~because large particles have large deposition velocities from the air of large particles. Air-surface exchange and petroleum residue account respectively for  
25 9% and 10% of ~~total PAHs in~~ accumulation mode PAHs mode aerosols whereas they ~~are plus~~ 30% and 27% in coarse mode aerosols PAHs. Note that the ~~concentrations contribution~~ of vehicle-derived PAHs (vehicular emission) are almost constant through all over the year, i.e. ~~it is contribute~~ 22% of ~~total PAHs in~~ accumulation mode PAHs aerosols whereas and ~~it is~~ 18% of ~~total PAHs in~~ coarse mode aerosols PAHs. In

~~combination with PAHs mode distribution, we know high level of PAHs occurring in accumulation mode particles. Together with Aitken mode particles, we can obtain 80% of PAHs from the contribution of fine particles (Aitken and accumulation mode particles). When taking the size distribution of the PAH into consideration, it can~~  
5 ~~conclude easily interpretable main emission sources for PAHs. As discussed above, most PAHs are characterized by a main peak in accumulation mode, suggesting that high concentration of PAHs occurred in fine particles. Additionally, concentrations of total PAHs in fine particles contribute to 80% of total concentrations in PM. Apparently, these PAHs mainly came from~~  
10 ~~Apparently, the presence of sources at or close to fine particulate level should be collectively responsible for this observation. Consequently, vehicle exhaust, coal combustion and biomass burning, are deemed three appreciable source of PAHs. Moreover, multiple emission mechanisms, i.e. vehicle exhaust, coal combustion and biomass burning tend to contribute fine particles, which largely adsorb PAHs that generated at the same time due to the large specific surface area, and results~~  
15 ~~in significantly higher concentrations of PAHs in fine particles than in coarse particles.~~

### 3.5 Respiratory exposure to PAHs

In order to assess deposition efficiency and flux of size-resolved PAHs in the human respiratory tract, we applied a so-called International Commission on Radiological Protection (ICRP) model (1994). More details on calculating from the model are  
20 included elsewhere (K. Zhang et al., 2012; Kawanaka et al., 2009). ~~Commonly, the respiratory tract is divided into three deposition regions: head airway (HA), tracheobronchial (TB), and alveolar region (AR).~~ The breath rate of normal people was considered at  $0.45 \text{ m}^3 \text{ h}^{-1}$ . ~~Figure 11~~ Fig. 10 shows the deposition fluxes of size-resolved PAHs and their relative contributions in the head, tracheobronchial and alveolar regions.  
25 Apparently, we can find a flux peak value in accumulation mode particles ( $1.1\text{-}2.1 \mu\text{m}$ ), similar to particle size distribution of PAHs as described previously (see section 3.1). The total PAHs deposition fluxes are  $8.8 \pm 2.0 \text{ ng h}^{-1}$ . ~~The mean value ( $8.8 \text{ ng h}^{-1}$ ) is which is 2.4 times~~ higher than that in indoor air of an urban community of Guangzhou, China ( $3.7 \text{ ng h}^{-1}$ ) (K. Zhang et al., 2012), ~~but it is.~~ ~~Conversely, the intake rate of total~~

PAHs is much lower than that for in a common traffic police in Beijing (280 ng h<sup>-1</sup> calculated by at the respiratory rate of 0.83 m<sup>3</sup> h<sup>-1</sup>) (Liu et al., 2007). Moreover, we find the relative PAHs abundance vary a lot with the particle size. In addition, through calculating the relative abundance of PAHs in each region, we can find that they change significantly over particle sizes. As When particle size increases, the relative PAHs abundance of PAHs increases in the head region increases, unchanges in tracheobronchial region, but decreases while in alveolar region, decreases. Note that the relative abundance of PAHs in tracheobronchial region is almost constant across all particle sizes, i.e. it is 6% from accumulation mode particles whereas it is 4% from coarse mode particles. These results indicate that coarse particles only contribute lots of PAHs in head region, while small fine particles contribute most PAHs in alveolar region. are major contributors to PAHs deposition in alveolar region. Furthermore, t These fine or ultrafine particles can also pass human lung rapidly into the systematic circulation, which may cause systematic exposure to PAHs (Nemmar et al., 2002).

Evaluating respiratory exposure need to incorporates considering the deposition efficiency of size-resolved PAHs. Deposition efficiency represents the deposition effectiveness of atmospheric PAHs in human respiratory tract. The efficiency can then be calculated by the formula of ICRP model. Figure 12 Fig. 11 shows the regional deposition efficiency of total PAHs across particle sizes. Generally, the total deposition efficiency of PAHs is found to increases with the particles size increases except for . However, in the alveolar region, in which the PAHs deposition efficiency increases with particle size decreases. This suggests that smaller particles can easily pass respiratory tract and deposit in alveolar region. the deposition efficiencies of total PAHs monotonously increased towards the smaller particles. This result suggests that the smaller particle can penetrate the respiratory tract and travel into the deeper alveolar region. This, combined with the fact that most 5- and 6 more-ring PAHs tend to adsorb on smaller particles, makes it them more important for potential health damage.

One We can utilize the LCR to estimate the exposure of PAHs through inhalation of ambient particles. From Fig. 13 12, shows that the LCR variations of the LCR from

~~of~~ normal (breath rate:  $0.45 \text{ m}^3 \text{ h}^{-1}$ ) and exercising people (breath rate:  $0.83 \text{ m}^3 \text{ h}^{-1}$ ) ~~across particle sizes during haze and non-haze periods can be identified.~~ The curve of LCR displays a unimodal distribution with only one distinct peak located at 1.1–2.1  $\mu\text{m}$ . ~~The size distribution of LCR is also unimodal with the maximum in the 1.1–2.1  $\mu\text{m}$  particle fraction.~~ LCR from the PAHs in a Accumulation mode PAHs particles contributes mainly about 54% of LCR, suggesting that total PAHs. ~~These data show that accumulation particles are major carcinogenic PAHs carriers for carcinogenic PAHs.~~ ~~Through the LCR~~ After calculation ~~from the exposure to particulate PAHs,~~ we can obtain that the LCR value is  $6.3(\pm 0.8) \times 10^{-7}$  of at normal respiratory condition ( $0.45 \text{ m}^3 \text{ h}^{-1}$ ) ~~a normal people is  $6.3(\pm 0.8) \times 10^{-7}$  during the Shanghai haze period,~~ which approaches to ~~is lower than~~ the cancer risk guideline value ( $10^{-6}$ ) (US EPA, 2005~~1989~~). ~~Here, it should be emphasized that LCR depended~~ As we known, the value of LCR depends strongly on the respiratory rate. ~~( $0.45 \text{ m}^3 \text{ h}^{-1}$  was utilized for normal condition).~~ ~~If we apply another an~~ average respiratory rate of  $0.83 \text{ m}^3 \text{ h}^{-1}$  (for ~~exercise~~ people who exercise outside) ~~applied by Liu et al. (Liu et al., 2007) was also used here,~~ ~~total the~~ LCR value will arrive at ~~would be~~  $1.2(\pm 0.2) \times 10^{-6}$ , which ~~approached or exceeded~~ exceeds the cancer risk guideline value, especially in severe haze days the value can reach up to ~~peaked at almost~~  $1.5 \times 10^{-6}$ . Note that this value is only from the size-resolved particulate PAHs, and responsible to part of respiratory risk to atmospheric PAHs. If the gaseous PAHs ~~were~~ are also taken into account, the cancer risk ~~would~~ will probably be even much ~~bigger~~ higher. ~~Furthermore, i~~ In combination with previous PMF source analysis ~~on size fractionated PAHs,~~ we find that the ~~higher cancer risk caused in accumulationed modes~~ sources of these PAHs mainly ~~resulted~~ come from biomass burning (24%), coal combustion (25%) and vehicular emission (27%). This is ~~consistent~~ Consistently with ~~our results,~~ the previous epidemiological studies ~~reported~~ that smaller particles ~~could~~ can ~~arouse~~ give rise to larger risk of cardiovascular toxicity through breathing (Pope et al., 2009). Thus, it appears to be important to perform more restrict control on smaller particles emission, particularly aiming at the reducing their releasing sources.

#### 4 Summary and conclusions

The overall conclusion of the present study is that it ~~We~~ systematically investigated the modal particle size distribution characteristics of PAHs ~~in at the~~ Shanghai urban atmosphere site and ~~identified~~ determined their emission source, ~~contribution to adverse~~ health effects through inhalation. It was ~~We~~ found that the size-resolved PAHs size distribution ~~have~~ exhibited a bimodal distribution pattern, with one mode peak (0.4-2.1  $\mu\text{m}$ ) in the fine mode size range (0.4-2.1  $\mu\text{m}$ ) and another peak ones (3.3-9  $\mu\text{m}$ ) in the coarse mode size range (3.3-9  $\mu\text{m}$ ). This present study proposes the ~~m~~Multiple adsorption and absorption mechanisms ~~controlling~~ controlled the behavior and fate of PAHs distribution among different sizes particles ~~considered as a function of size~~. Further calculations using ~~inhaling particle-bound PAHs data showed~~ ~~t~~The estimated LCR value for people who exercise outside was  $1.2(\pm 0.2) \times 10^{-6}$ , which exceeded ~~were~~ bigger than the cancer risk guideline value ( $10^{-6}$ ), ~~especially for people exercising during haze days ( $1.5 \times 10^{-6}$ )~~. Accumulation mode PAHs contributed about 54% of LCR. Based on PMF results, their sources ~~The largest contribution for LCR mainly came from PAHs on accumulation particles, and mainly resulted~~ came from biomass burning (24%), coal combustion (25%) and vehicular emission (27%). ~~The~~ This findings ~~presented here~~ study could provide a preliminary data for developing effective strategies for source control.

#### 20 Acknowledgments.

This work was supported by the National Natural Science Foundation of China (Nos. 21577021, 21177025, 21377028, 41475109), the Excellent Academic Leader Program (No. 14XD1400600), FP720 project (AMIS, IRSES-GA-2011) and the Major Research Project (No. 12DJ1400100) of Science and Technology Commission of Shanghai Municipality.

#### References

Akyuz, M., and Cabuk, H.: Meteorological variations of PM<sub>2.5</sub>/PM<sub>10</sub> concentrations and particle-associated polycyclic aromatic hydrocarbons in the atmospheric environment of Zonguldak, Turkey, J. Hazard. Mater., 170, 13-21, 2009.

- Allen, J. O., Dookeran, K. M., Smith, K. A., Sarofim, A. F., Taghizadeh, K., and Lafleur, A. L.: Measurement of polycyclic aromatic hydrocarbons associated with size-segregated atmospheric aerosols in Massachusetts, *Environ. Sci. Technol.*, 30, 1023-1031, 1996.
- 5 [Arhami, M., Minguillón, M. C., Polidori, A., Schauer, J. J., Delfino, R. J., and Sioutas, C.: Organic compound characterization and source apportionment of indoor and outdoor quasi-ultrafine particulate matter in retirement homes of the Los Angeles Basin, \*Indoor Air\*, 20, 17-30, 2010.](#)
- Bi, X., Sheng, G., Peng, P. ~~A~~, Chen, Y., and Fu, J.: Size distribution of n-alkanes and polycyclic aromatic hydrocarbons (PAHs) in urban and rural atmospheres of Guangzhou, China, *Atmos. Environ.*, 39, 477-487, 2005.
- 10 Bostrom, C. E., Gerde, P., Hanberg, A., Jernstrom, B., Johansson, C., Kyrklund, T., Rannug, A., Tornqvist, M., Victorin, K., and Westerholm, R.: Cancer risk assessment, indicators, and guidelines for polycyclic aromatic hydrocarbons in the ambient air, *Environ. Health Perspect.*, 110, 451-488, 2002.
- 15 Chan, A. W. H., Kautzman, K. E., Chhabra, P. S., Surratt, J. D., Chan, M. N., Crouse, J. D., Kürten, A., Wennberg, P. O., Flagan, R. C., and Seinfeld, J. H.: Secondary organic aerosol formation from photooxidation of naphthalene and alkylnaphthalenes: implications for oxidation of intermediate volatility organic compounds (IVOCs), *Atmos. Chem. Phys.*, 9, 3049-3060, doi:10.5194/acp-9-3049-2009, 2009.
- 20 Chen, S. C., and Liao, C. M.: Health risk assessment on human exposed to environmental polycyclic aromatic hydrocarbons pollution sources, *Sci. Total Environ.*, 366, 112-123, 2006.
- Delgado-Saborit, J. M., Stark, C., and Harrison, R. M.: Use of a Versatile High Efficiency Multiparallel Denuder for the Sampling of PAHs in Ambient Air: Gas and Particle Phase Concentrations, Particle Size Distribution and Artifact Formation, *Environ. Sci. Technol.*, 48, 499-507, 2013.
- 25 Ding, X., Wang, X.M., Xie, Z.Q., Xiang, C.H., Mai, B.X., Sun, L.G., Zheng, M., Sheng, G.Y., Fu, J.M., and Pöschl, U.: Atmospheric polycyclic aromatic hydrocarbons observed over the North Pacific Ocean and the Arctic area: Spatial distribution and source identification, *Atmos. Environ.*, 41, 2061-2072, 2007.
- 30 Duan, J. C., Bi, X. H., Tan, J. H., Sheng, G. Y., and Fu, J. M.: The differences of the size distribution of polycyclic aromatic hydrocarbons (PAHs) between urban and rural sites of Guangzhou, China, *Atmos. Res.*, 78, 190-203, 2005.
- Duan, J. C., Bi, X. H., Tan, J. H., Sheng, G. Y., and Fu, J. M.: Seasonal variation on size distribution and concentration of PAHs in Guangzhou city, China, *Chemosphere*, 67, 614-622, 2007.
- 35 Fernández, P., Grimalt, J. O., and Vilanova, R. M.: Atmospheric Gas-Particle Partitioning of Polycyclic Aromatic Hydrocarbons in High Mountain Regions of Europe, *Environ. Sci. Technol.*, 36, 1162-1168, 2002.
- Garrido, A., Jimenez-Guerrero, P., and Ratola, N.: Levels, trends and health concerns of atmospheric PAHs in Europe, *Atmos. Environ.*, 99, 474-484, 2014.



- Geiser, M., Rothen-Rutishauser, B., Kapp, N., Schurch, S., Kreyling, W., Schulz, H., Semmler, M., Hof, V. I., Heyder, J., and Gehr, P.: Ultrafine particles cross cellular membranes by nonphagocytic mechanisms in lungs and in cultured cells, *Environ. Health Perspect.*, 113, 1555-1560, 2005.
- 5 Gigliotti, C. L., Brunciak, P. A., Dachs, J., Glenn, T. R., Nelson, E. D., Totten, L. A., and Eisenreich, S. J.: Air-water exchange of polycyclic aromatic hydrocarbons in the New York-New Jersey, Usa, Harbor Estuary, *Environ. Toxicol. Chem.*, 21, 235-244, 2002.
- Gnauk, T., Muller, K., Bruggemann, E., Birmili, W., Weinhold, K., van Pinxteren, D., Loschau, G., Spindler, G., and Herrmann, H.: A study to discriminate local, urban and regional source  
10 contributions to the particulate matter concentrations in the city of Dresden, Germany, *J. Atmos. Chem.*, 68, 199-231, 2011.
- Gupta, S., Kumar, K., Srivastava, A., Srivastava, A., and Jain, V. K.: Size distribution and source apportionment of polycyclic aromatic hydrocarbons (PAHs) in aerosol particle samples from the atmospheric environment of Delhi, India, *Sci. Total Environ.*, 409, 4674-4680, 2011.
- 15 Harrison, R. M., Smith, D. J. T., and Luhana, L.: Source apportionment of atmospheric polycyclic aromatic hydrocarbons collected from an urban location in Birmingham, UK, *Environ. Sci. Technol.*, 30, 825-832, 1996.
- Hien, T. T., Thanh, L. T., Kameda, T., Takenaka, N., and Bandow, H.: Distribution characteristics of polycyclic aromatic hydrocarbons with particle size in urban aerosols at the roadside in Ho Chi  
20 Minh City, Vietnam, *Atmos. Environ.*, 41, 1575-1586, 2007.
- Hytönen, K., Yli-Pirilä P., Tissari, J., Gröhn, A., Riipinen, I., Lehtinen, K. E. J., and Jokiniemi, J.: Gas-Particle Distribution of PAHs in Wood Combustion Emission Determined with Annular Denuders, Filter, and Polyurethane Foam Adsorbent, *Aerosol Sci. Technol.*, 43, 442-454, 2009.
- International Commission on Radiological Protection (ICRP): Human respiratory tract model for  
25 radiological protection, Publication 66, Elsevier Science, Oxford, UK, 1994.
- Kameda, Y., Shirai, J., Komai, T., Nakanishi, J., and Masunaga, S.: Atmospheric polycyclic aromatic hydrocarbons: size distribution, estimation of their risk and their depositions to the human respiratory tract, *Sci. Total Environ.*, 340, 71-80, 2005.
- Kamens, R., Jang, M., Chien, C. J., and Leach, K.: Aerosol formation from the reaction of alpha-pinene and ozone using a gas-phase kinetics aerosol partitioning model, *Environ. Sci. Technol.*,  
30 33, 1430-1438, 1999.
- Kamens, R. M., and Jaoui, M.: Modeling aerosol formation from alpha-pinene plus NO<sub>x</sub> in the presence of natural sunlight using gas-phase kinetics and gas-particle partitioning theory, *Environ. Sci. Technol.*, 35, 1394-1405, 2001.
- 35 Kavouras, I. G., Mihalopoulos, N., and Stephanou, E. G.: Secondary organic aerosol formation vs primary organic aerosol emission: In situ evidence for the chemical coupling between monoterpene acidic photooxidation products and new particle formation over forests, *Environ. Sci. Technol.*, 33, 1028-1037, 1999.

- Kawanaka, Y., Matsumoto, E., Sakamoto, K., Wang, N., and Yun, S. J.: Size distributions of mutagenic compounds and mutagenicity in atmospheric particulate matter collected with a low-pressure cascade impactor, *Atmos. Environ.*, 38, 2125-2132, 2004.
- 5 Kawanaka, Y., Tsuchiya, Y., Yun, S.-J., and Sakamoto, K.: Size Distributions of Polycyclic Aromatic Hydrocarbons in the Atmosphere and Estimation of the Contribution of Ultrafine Particles to Their Lung Deposition, *Environ. Sci. Technol.*, 43, 6851-6856, 2009.
- Keshtkar, H., and Ashbaugh, L. L.: Size distribution of polycyclic aromatic hydrocarbon particulate emission factors from agricultural burning, *Atmos. Environ.*, 41, 2729-2739, 2007.
- 10 Kong, S., Lu, B., Ji, Y., Bai, Z., Xu, Y., Liu, Y., and Jiang, H.: Distribution and sources of polycyclic aromatic hydrocarbons in size-differentiated re-suspended dust on building surfaces in an oilfield city, China, *Atmos. Environ.*, 55, 7-16, 2012.
- 15 Kong, S. F., Shi, J. W., Lu, B., Qiu, W. G., Zhang, B. S., Peng, Y., Zhang, B. W., and Bai, Z. P.: Characterization of PAHs within PM10 fraction for ashes from coke production, iron smelt, heating station and power plant stacks in Liaoning Province, China, *Atmos. Environ.*, 45, 3777-3785, 2011.
- Ladji, R., Yassaa, N., Balducci, C., and Cecinato, A.: Particle size distribution of n-alkanes and polycyclic aromatic hydrocarbons (PAHS) in urban and industrial aerosol of Algiers, Algeria, *Environ. Sci. Pollut. Res.*, 21, 1819-1832, 2014.
- 20 Larsen, R. K., and Baker, J. E.: Source apportionment of polycyclic aromatic hydrocarbons in the urban atmosphere: A comparison of three methods, *Environ. Sci. Technol.*, 37, 1873-1881, 2003.
- Lee, J. Y., Shin, H. J., Bae, S. Y., Kim, Y. P., and Kang, C. H.: Seasonal variation of particle size distributions of PAHs at Seoul, Korea, *Air Qual. Atmos. Hlth.*, 1, 57-68, 2008.
- 25 Li, J., Zhang, G., Li, X. D., Qi, S. H., Liu, G. Q., and Peng, X. Z.: Source seasonality of polycyclic aromatic hydrocarbons (PAHs) in a subtropical city, Guangzhou, South China, *Sci. Total Environ.*, 355, 145-155, 2006.
- Li, P. F., Li, X., Yang, C. Y., Wang, X. J., Chen, J. M., and Collett, J. L.: Fog water chemistry in Shanghai, *Atmos. Environ.*, 45, 4034-4041, 2011.
- Li, X., Li, P., Yan, L., Chen, J., Cheng, T., and Xu, S.: Characterization of polycyclic aromatic hydrocarbons in fog-rain events, *J. Environ. Monit.*, 13, 2988-2993, 2011.
- 30 Lin, T., Hu, L. M., Guo, Z. G., Qin, Y. W., Yang, Z. S., Zhang, G., and Zheng, M.: Sources of polycyclic aromatic hydrocarbons to sediments of the Bohai and Yellow Seas in East Asia, *J. Geophys. Res.*, 116, D23305, doi:10.1029/2011jd015722, 2011.
- Lindgren, F., Geladi, P., Berglund, A., Sjoström, M., and Wold, S.: Interactive Variable Selection (Ivs) for Pls .2. Chemical Applications, *J. Chemometr.*, 9, 331-342, 1995.
- 35 Liu, Y. N., Tao, S., Dou, H., Zhang, T. W., Zhang, X. L., and Dawson, R.: Exposure of traffic police to Polycyclic aromatic hydrocarbons in Beijing, China, *Chemosphere*, 66, 1922-1928, 2007.
- Ma, W. L., Li, Y. F., Qi, H., Sun, D. Z., Liu, L. Y., and Wang, D. G.: Seasonal variations of sources

- of polycyclic aromatic hydrocarbons (PAHs) to a northeastern urban city, China, *Chemosphere*, 79, 441-447, 2010.
- 5 Mai, B. X., Qi, S. H., Zeng, E. Y., Yang, Q. S., Zhang, G., Fu, J. M., Sheng, G. Y., Peng, P. N., and Wang, Z. S.: Distribution of polycyclic aromatic hydrocarbons in the coastal region off Macao, China: Assessment of input sources and transport pathways using compositional analysis, *Environ. Sci. Technol.*, 37, 4855-4863, 2003.
- McWhinney, R. D., Zhou, S., and Abbatt, J. P. D.: Naphthalene SOA: redox activity and naphthoquinone gas-particle partitioning, *Atmos. Chem. Phys.*, 13, 9731-9744, doi:10.5194/acp-13-9731-2013, 2013.
- 10 Mesquita, S. R., van Drooge, B. L., Reche, C., Guimarães, L., Grimalt, J. O., Barata, C., and Piñá, B.: Toxic assessment of urban atmospheric particle-bound PAHs: Relevance of composition and particle size in Barcelona (Spain), *Environ. Pollut.*, 184, 555-562, 2014.
- Miguel, A. H., Eiguren-Fernandez, A., Jaques, P. A., Froines, J. R., Grant, B. L., Mayo, P. R., and Sioutas, C.: Seasonal variation of the particle size distribution of polycyclic aromatic hydrocarbons and of major aerosol species in Claremont, California, *Atmos. Environ.*, 38, 3241-3251, 2004.
- 15 Nemmar, A., Hoet, P. H. M., Vanquickenborne, B., Dinsdale, D., Thomeer, M., Hoylaerts, M. F., Vanbilloen, H., Mortelmans, L., and Nemery, B.: Passage of inhaled particles into the blood circulation in humans, *Circulation*, 105, 411-414, 2002.
- 20 [Nisbet, I. C. T., and Lagoy, P. K.: Toxic equivalency factors \(TEFs\) for polycyclic aromatic hydrocarbons \(PAHs\), \*Regul. Toxicol. Pharm.\*, 16, 290-300, 1992.](#)
- Offenberg, J. H., and Baker, J. E.: Aerosol Size Distributions of Polycyclic Aromatic Hydrocarbons in Urban and Over-Water Atmospheres, *Environ. Sci. Technol.*, 33, 3324-3331, 1999.
- 25 Oliveira, C., Martins, N., Tavares, J., Pio, C., Cerqueira, M., Matos, M., Silva, H., Oliveira, C., and Camoes, F.: Size distribution of polycyclic aromatic hydrocarbons in a roadway tunnel in Lisbon, Portugal, *Chemosphere*, 83, 1588-1596, 2011.
- Paatero, P. and Tapper, U.: Positive Matrix Factorization - a Nonnegative Factor Model with Optimal Utilization Of Error-Estimates Of Data Values, *Environmetrics*, 5, 111-126, doi:10.1002/env.3170050203, 1994.
- 30 Pope, C. A., Ezzati, M., and Dockery, D. W.: Fine-Particulate Air Pollution and Life Expectancy in the United States, *New Engl. J. Med.*, 360, 376-386, 2009.
- Poulain, L., Iinuma, Y., Müller, K., Birmili, W., Weinhold, K., Brüggemann, E., Gnauk, T., Hausmann, A., Löschau, G., Wiedensohler, A., and Herrmann, H.: Diurnal variations of ambient particulate wood burning emissions and their contribution to the concentration of Polycyclic Aromatic Hydrocarbons (PAHs) in Seiffen, Germany, *Atmos. Chem. Phys.*, 11, 12697-12713, doi:10.5194/acp-11-12697-2011, 2011.
- 35 Ravindra, K., Sokhi, R., and Van Grieken, R.: Atmospheric polycyclic aromatic hydrocarbons: Source attribution, emission factors and regulation, *Atmos. Environ.*, 42, 2895-2921, 2008.

- Sanderson, E. G., and Farant, J. P.: Atmospheric Size Distribution of PAHs: Evidence of a High-Volume Sampling Artifact, *Environ. Sci. Technol.*, 39, 7631-7637, 2005.
- Sheesley, R. J., Krusa, M., Krecl, P., Johansson, C., and Gustafsson, O.: Source apportionment of elevated wintertime PAHs by compound-specific radiocarbon analysis, *Atmos. Chem. Phys.*, 9, 3347-3356, doi:10.5194/acp-9-3347-2009, 2009.
- Shen, G., Wang, W., Yang, Y., Ding, J., Xue, M., Min, Y., Zhu, C., Shen, H., Li, W., Wang, B., Wang, R., Wang, X., Tao, S., and Russell, A. G.: Emissions of PAHs from Indoor Crop Residue Burning in a Typical Rural Stove: Emission Factors, Size Distributions, and Gas-Particle Partitioning, *Environ. Sci. Technol.*, 45, 1206-1212, 2011.
- Sofowote, U. M., McCarry, B. E., and Marvin, C. H.: Source apportionment of PAH in Hamilton Harbour suspended sediments: Comparison of two factor analysis methods, *Environ. Sci. Technol.*, 42, 6007-6014, 2008.
- Theodosi, C., Grivas, G., Zarmas, P., Chaloulakou, A., and Mihalopoulos, N.: Mass and chemical composition of size-segregated aerosols (PM1, PM2.5, PM10) over Athens, Greece: local versus regional sources, *Atmos. Chem. Phys.*, 11, 11895-11911, doi:10.5194/acp-11-11895-2011, 2011.
- [Teixeira, E. C., Agudelo-Castañeda, D. M., Fachel, J. M. G., Leal, K. L., Garcia, K. O., and Wiegand, F.: Source identification and seasonal variation of polycyclic aromatic hydrocarbons associated with atmospheric fine and coarse particles in the metropolitan area of Porto Alegre, RS, Brazil. \*Atmos. Res.\*, 118, 390-403, 2012b.](#)
- US EPA (U.S. Environmental Protection Agency): Risk assessment guidance for super fund volume I human health evaluation manual, part A, EPA/540/1-89/002, Office of Emergency and Remedial Response, Washington, D.C, USA, 1989.
- [US EPA \(U.S. Environmental Protection Agency\): Guidelines for carcinogen risk assessment. EPA/630/P-03/001F, Risk Assessment Forum, Washington, D.C, USA, 2005.](#)
- van Drooge, B. L., and Ballesta, P. P.: Seasonal and Daily Source Apportionment of Polycyclic Aromatic Hydrocarbon Concentrations in PM10 in a Semirural European Area, *Environ. Sci. Technol.*, 43, 7310-7316, 2009.
- Venkataraman, C., and Friedlander, S. K.: Size Distributions of Polycyclic Aromatic-Hydrocarbons and Elemental Carbon. 2. Ambient Measurements and Effects of Atmospheric Processes, *Environ. Sci. Technol.*, 28, 563-572, 1994.
- Venkataraman, C., Lyons, J. M., and Friedlander, S. K.: Size Distributions of Polycyclic Aromatic-Hydrocarbons and Elemental Carbon. 1. Sampling, Measurement Methods, and Source Characterization, *Environ. Sci. Technol.*, 28, 555-562, 1994.
- Venkataraman, C., Thomas, S., and Kulkarni, P.: Size distributions of polycyclic aromatic hydrocarbons - Gas/particle partitioning to urban aerosols, *J. Aerosol Sci*, 30, 759-770, 1999.
- Venkataraman, C., Negi, G., Sardar, S. B., and Rastogi, R.: Size distributions of polycyclic aromatic hydrocarbons in aerosol emissions from biofuel combustion, *J. Aerosol Sci*, 33, 503-518, 2002.
- Wang, G., Kawamura, K., Xie, M., Hu, S., Gao, S., Cao, J., An, Z., and Wang, Z.: Size-distributions

of n-alkanes, PAHs and hopanes and their sources in the urban, mountain and marine atmospheres over East Asia, *Atmos. Chem. Phys.*, 9, 8869-8882, doi:10.5194/acp-9-8869-2009, 2009.

5 Wang, X., Chen, J., Cheng, T., Zhang, R., and Wang, X.: Particle number concentration, size distribution and chemical composition during haze and photochemical smog episodes in Shanghai, *J. Environ. Sci.-China*, 26, 1894-1902, 2014.

Wilson, J. G., Kingham, S., Pearce, J., and Sturman, A. P.: A review of intraurban variations in particulate air pollution: Implications for epidemiological research, *Atmos. Environ.*, 39, 6444-6462, 2005.

10 Wu, D., Wang, Z., Chen, J., Kong, S., Fu, X., Deng, H., Shao, G., and Wu, G.: Polycyclic aromatic hydrocarbons (PAHs) in atmospheric PM<sub>2.5</sub> and PM<sub>10</sub> at a coal-based industrial city: Implication for PAH control at industrial agglomeration regions, China, *Atmos. Res.*, 149, 217-229, 2014.

15 Wu, S. P., Tao, S., and Liu, W. X.: Particle size distributions of polycyclic aromatic hydrocarbons in rural and urban atmosphere of Tianjin, China, *Chemosphere*, 62, 357-367, 2006.

Yang, H. H., Lai, S. O., Hsieh, L. T., Hsueh, H. J., and Chi, T. W.: Profiles of PAH emission from steel and iron industries, *Chemosphere*, 48, 1061-1074, 2002.

20 Yu, H., and Yu, J. Z.: Polycyclic aromatic hydrocarbons in urban atmosphere of Guangzhou, China: Size distribution characteristics and size-resolved gas-particle partitioning, *Atmos. Environ.*, 54, 194-200, 2012.

Yu, J. Z., Cocker, D. R., Griffin, R. J., Flagan, R. C., and Seinfeld, J. H.: Gas-phase ozone oxidation of monoterpenes: Gaseous and particulate products, *J. Atmos. Chem.*, 34, 207-258, 1999.

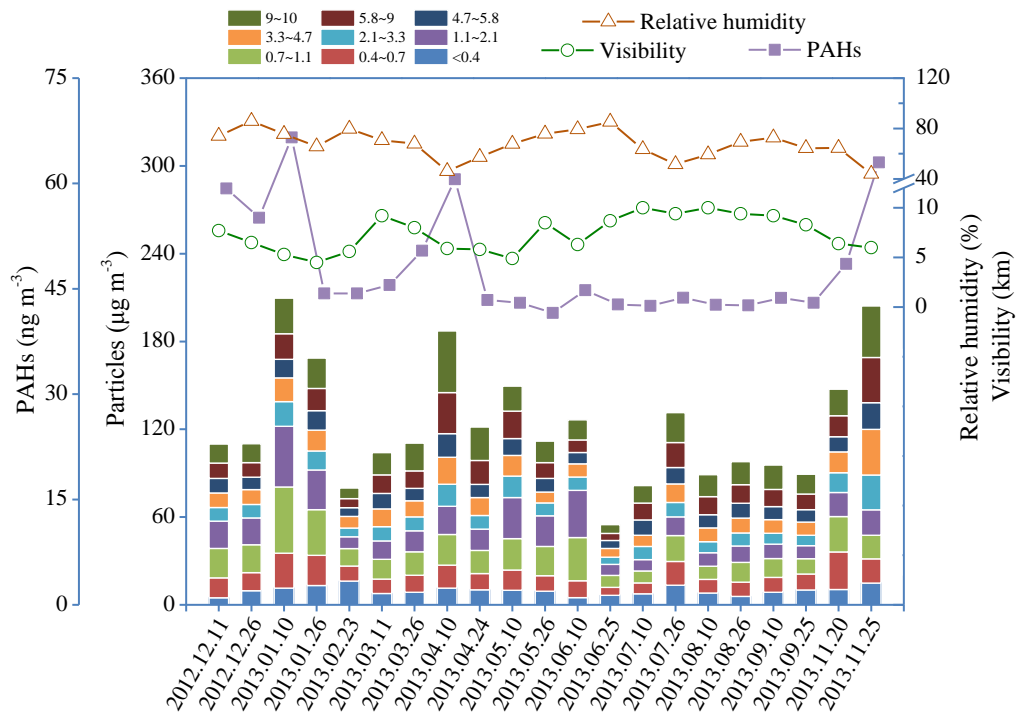
25 Zakaria, M. P., Takada, H., Tsutsumi, S., Ohno, K., Yamada, J., Kouno, E., and Kumata, H.: Distribution of polycyclic aromatic hydrocarbons (PAHs) in rivers and estuaries in Malaysia: A widespread input of petrogenic PAHs, *Environ. Sci. Technol.*, 36, 1907-1918, 2002.

Zhang, K., Zhang, B.Z., Li, S.M., Wong, C. S., and Zeng, E. Y.: Calculated respiratory exposure to indoor size-fractioned polycyclic aromatic hydrocarbons in an urban environment, *Sci. Total Environ.*, 431, 245-251, 2012a.

30 ~~Zhang, K., Zhang, B. Z., Li, S. M., Wong, C. S., and Zeng, E. Y.: Calculated respiratory exposure to indoor size-fractioned polycyclic aromatic hydrocarbons in an urban environment, *Sci. Total Environ.*, 431, 245-251, 10.1016/j.scitotenv.2012.05.059, 2012b.~~

Zhang, R., Khalizov, A., Wang, L., Hu, M., and Xu, W.: Nucleation and growth of nanoparticles in the atmosphere, *Chem Rev*, 112, 1957-2011, 10.1021/cr2001756, 2012.

35 Zhou, J. B., Wang, T. G., Zhang, Y. P., Mao, T., Huang, Y. B., Zhong, N. N., and Simoneit, B. R. T.: Sources and seasonal changes in the distributions of aliphatic and polycyclic aromatic hydrocarbons in size fractions of atmospheric particles of Beijing, China, *Environ Eng Sci*, 25, 207-220, 2008.



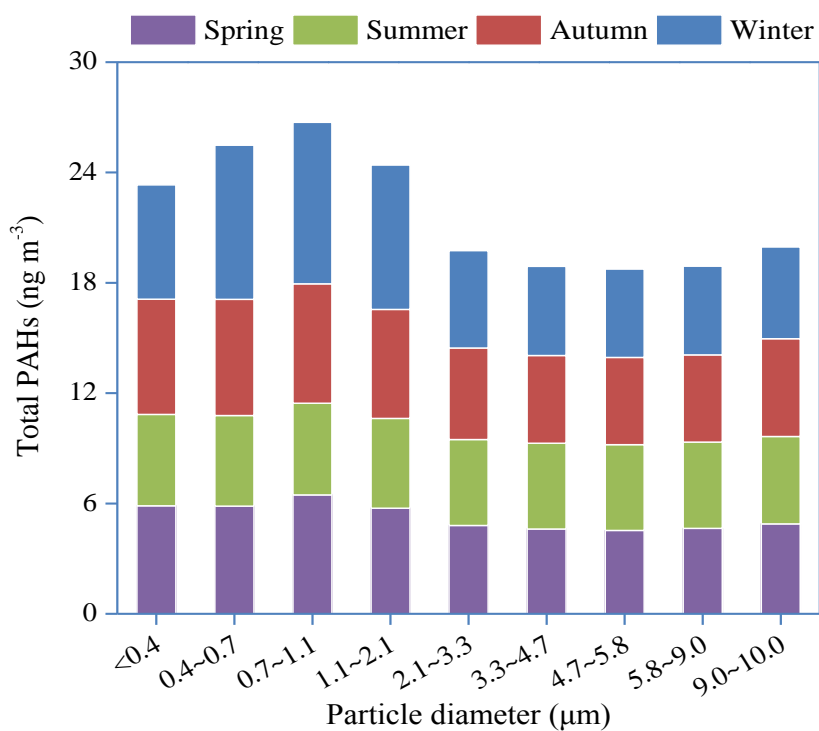
5 **Figure Fig. 1.** The sampling time series of PAH concentration ( $\text{ng m}^{-3}$ ), size-segregated particles ( $\mu\text{g m}^{-3}$ ), temperature ( $^{\circ}\text{C}$ ), visibility (km) and relative humidity (%).

10

15

20

25



5

**Figure 2.** Seasonal variation of size-segregated total PAHs.

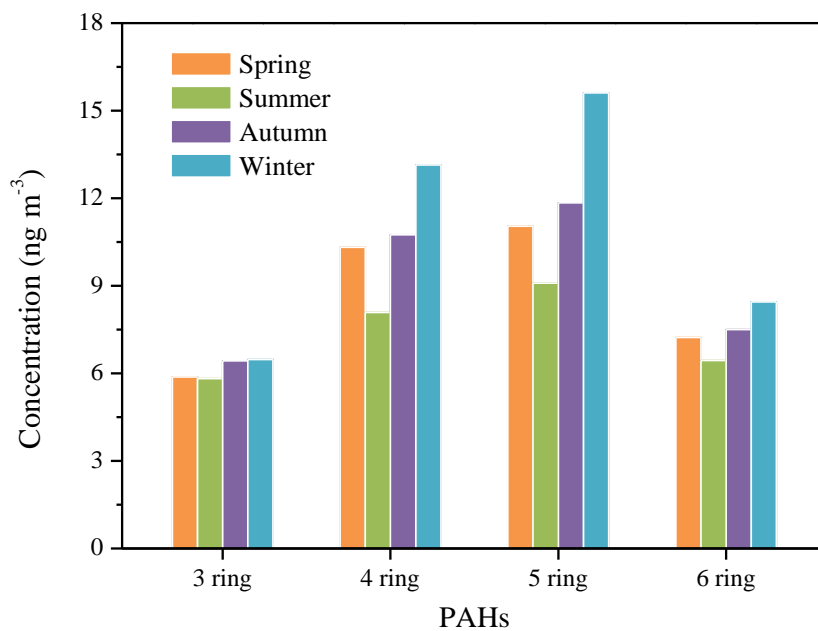
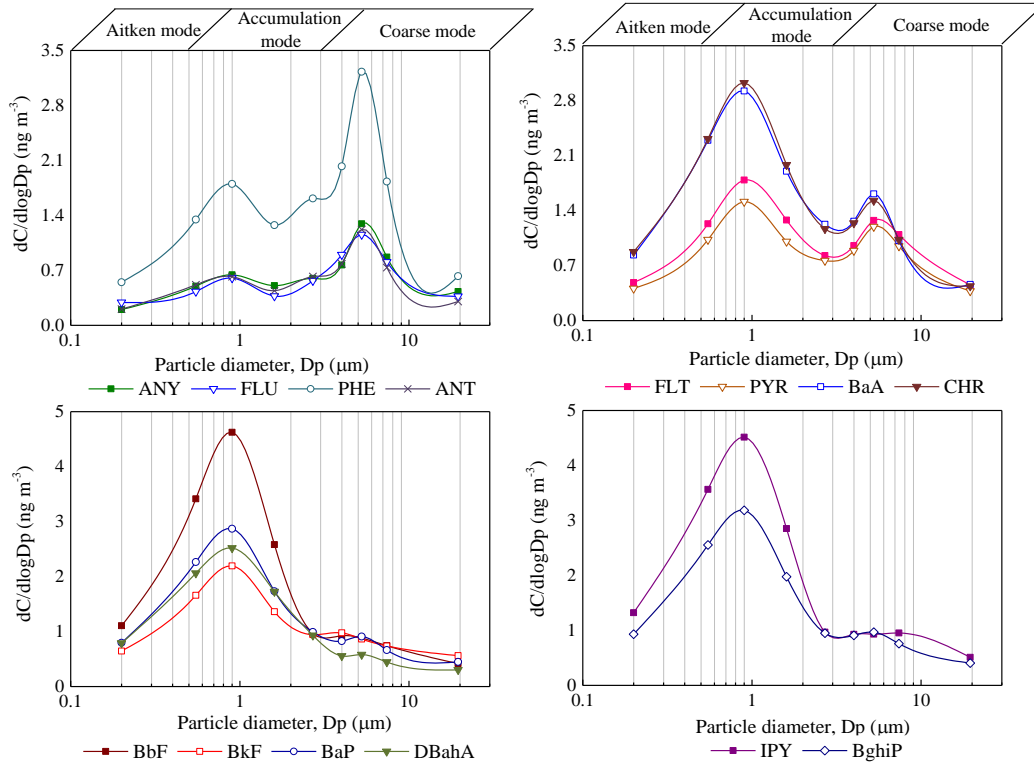


**Fig. 2.** Seasonal variation of 3 to 6 ring PAHs.

10



5

**Fig. 3. Particle size-size distributions of particle-bound PAHs (3 to 6 rings) in the atmosphere across one year for all samples.** dC is the concentration on each filter, C is the sum concentration on all filters, and  $d\log D_p$  is the logarithmic size interval for each impactor stage in aerodynamic diameter ( $D_p$ ).

10

15

20



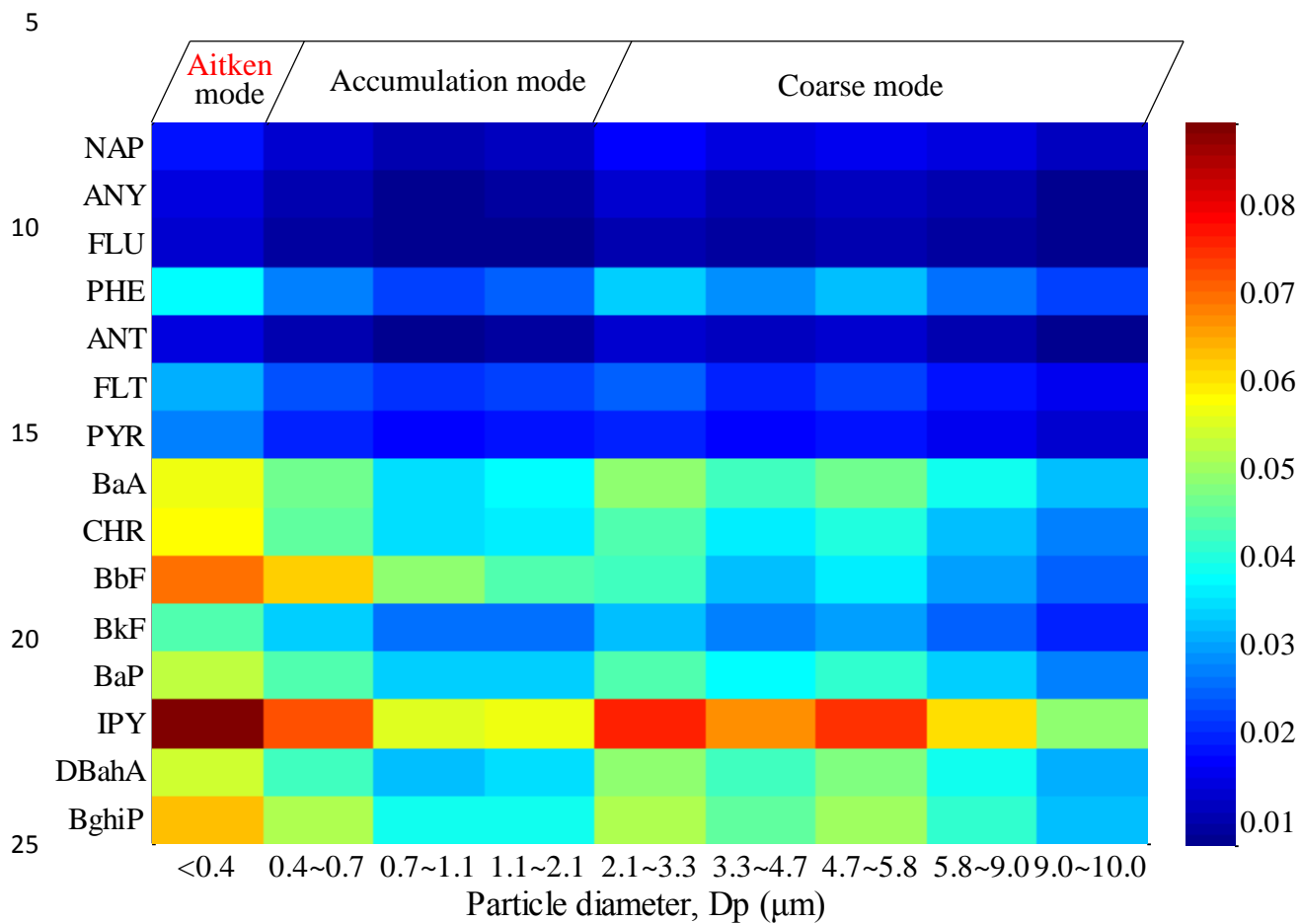
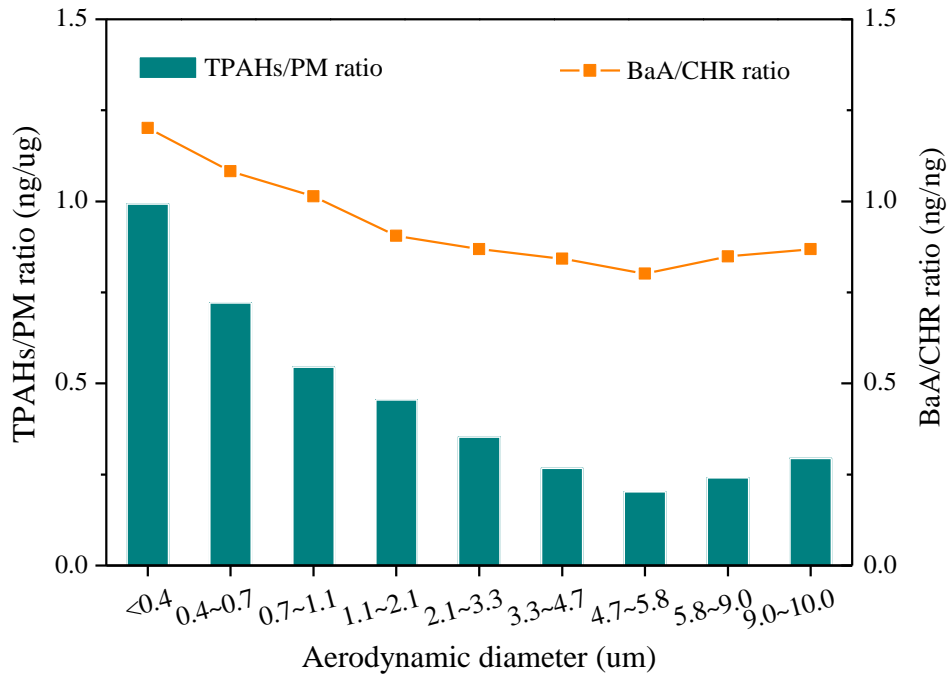


**Figure 4.** Mass Ratios of PAH species to size-segregated particles ( $\text{ng } \mu\text{g}^{-1}$ ) across all samples.

30

35

40



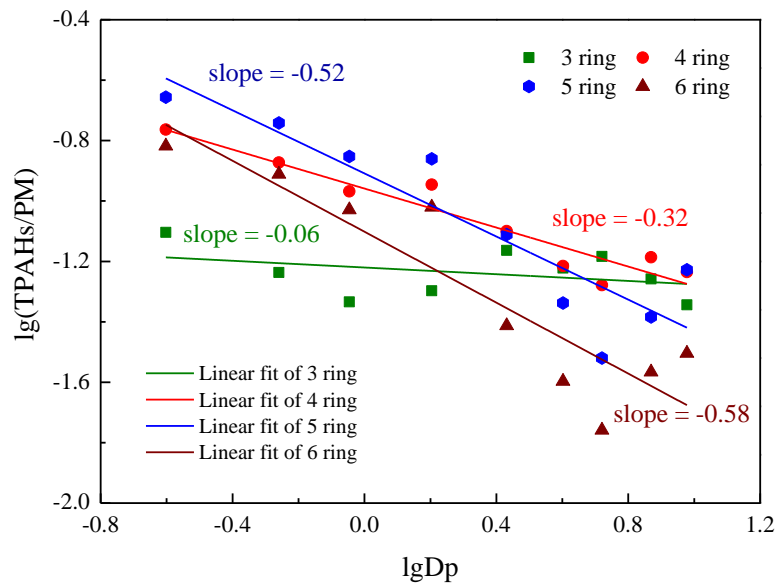
5 **Figure 5 Fig. 4.** Ratios of total PAHs/PM ~~size segregated particles~~ (ng  $\mu\text{g}^{-1}$ ) and BaA/CHR across particle sizes.

10

15

20

25



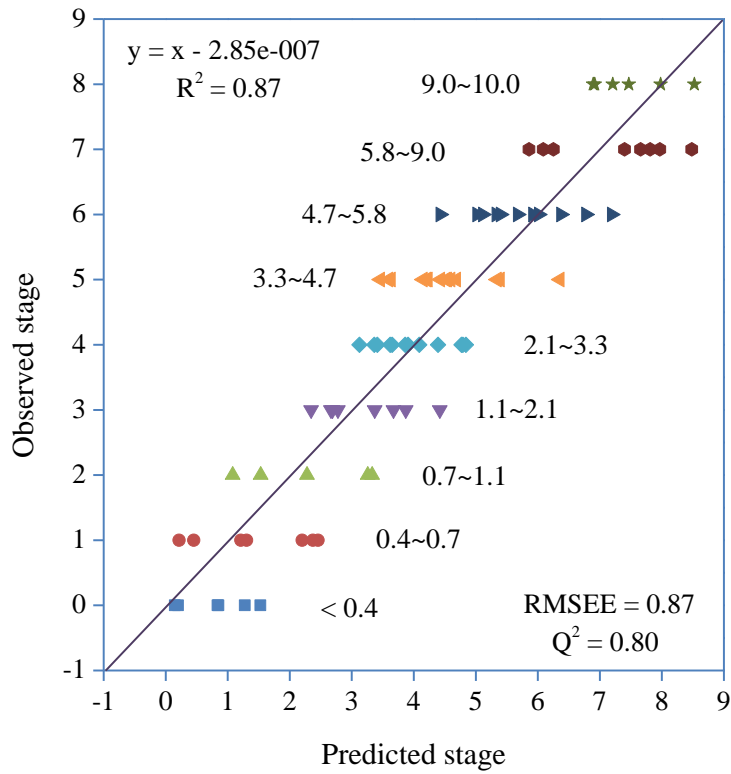
5 **Figure 6** **Fig. 5.** Plots of  $\lg(\text{TPAHs}/\text{PM}) - \lg(D_p)$  for PAHs with different ring number.

10

15

20

25

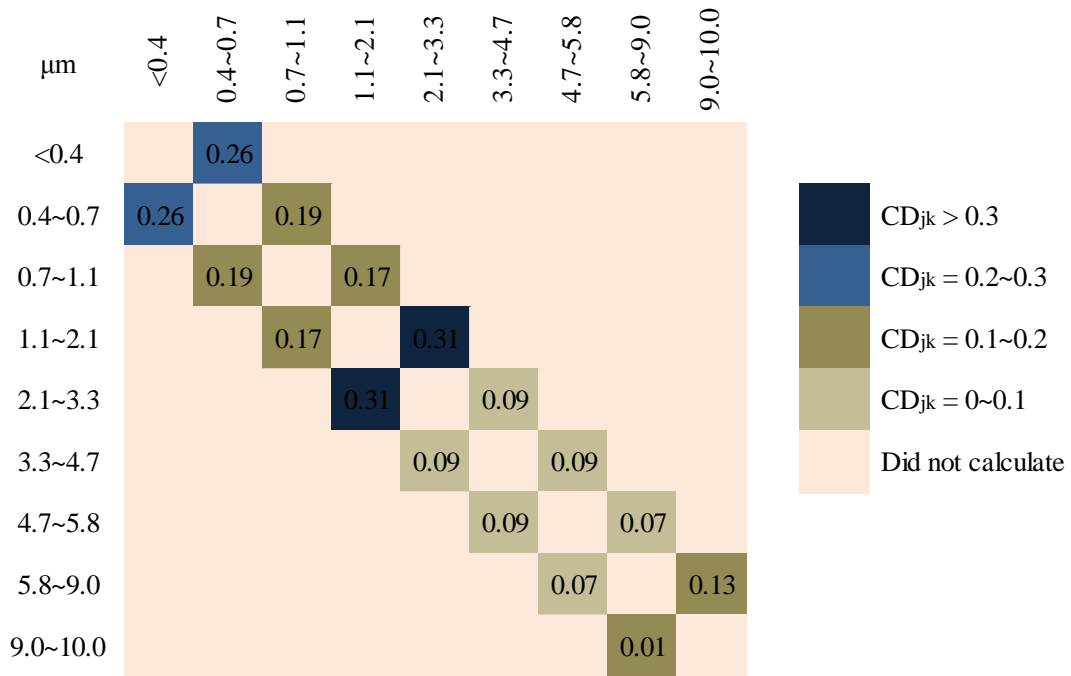


5 **Figure 7** **Fig. 6.** Measured and predicted total PAHs in all particles with sizes ranges from  $<0.4 \mu\text{m}$  to  $10 \mu\text{m}$ . The dashed line represents the  $45^\circ$  line.

10

15

20



5

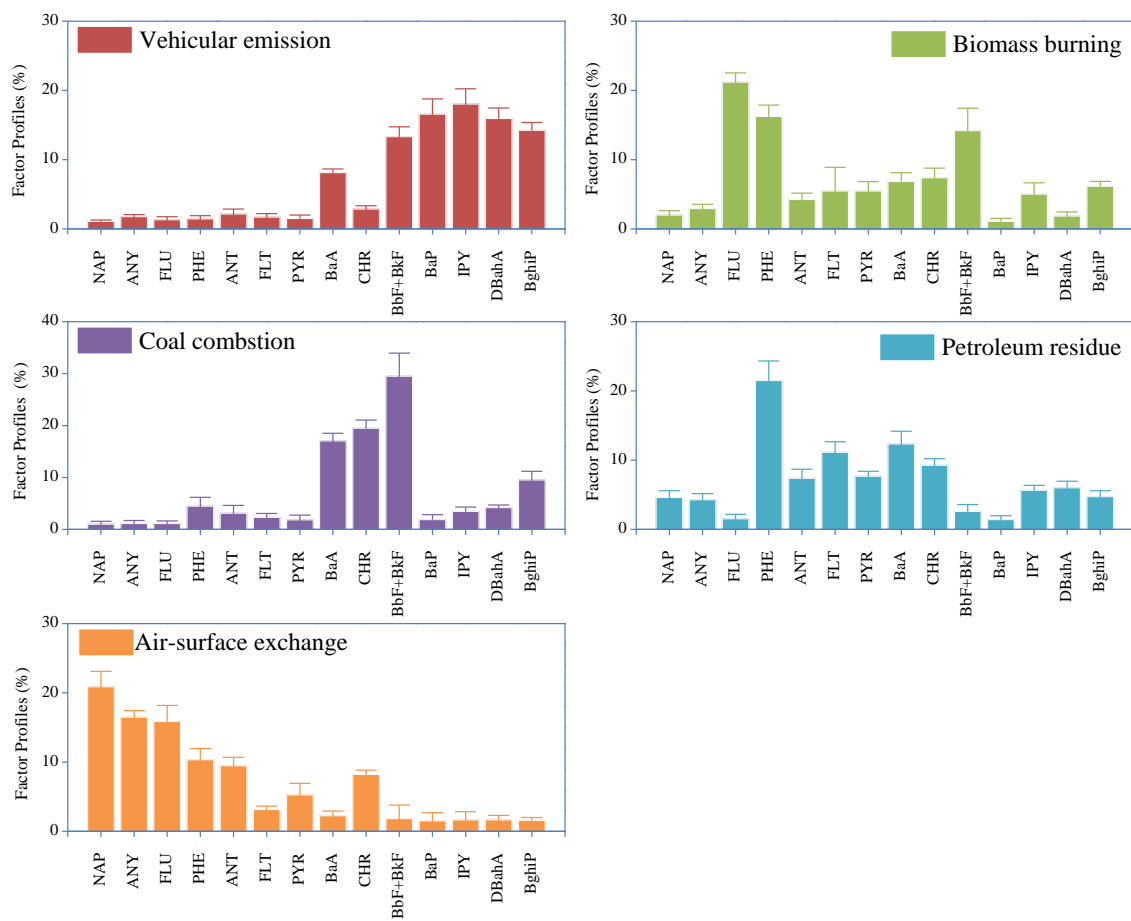
**Figure 8 Fig. 7.** Similar comparison of PAHs profiles for the adjacent particles fractions.

10

15

20

25

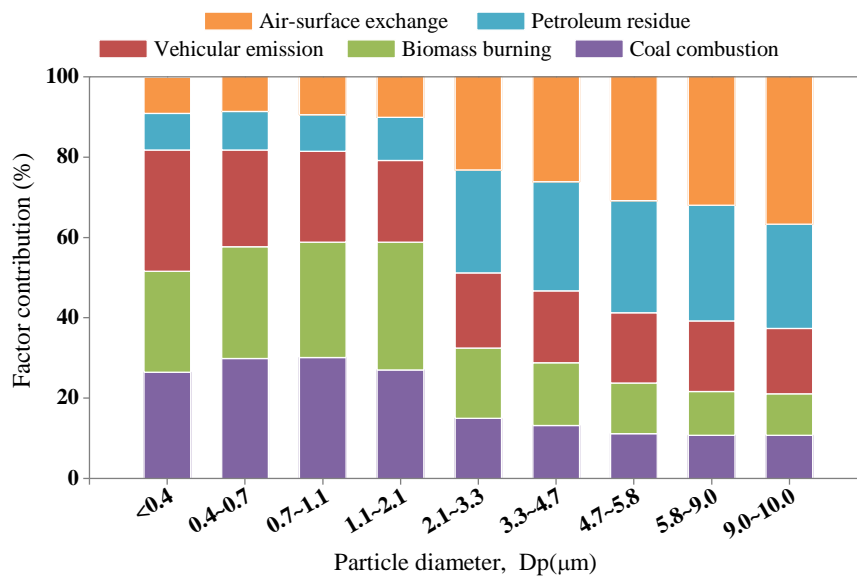


5 **Figure 9 Fig. 8.** Profiles of the five factors resolved by the PMF model from full-all PAHs data set.

10

15

20



5

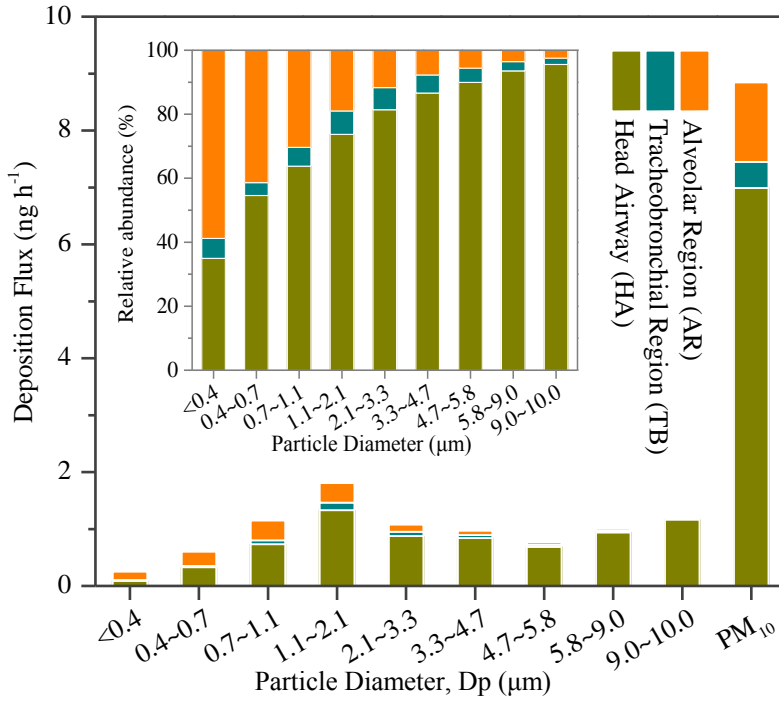
**Figure 10 Fig. 9.** Factor contributions to size-segregated particles by the PMF model from full PAHs data set.

10

15

20

25



5

**Figure 11 Fig. 10.** Deposition fluxes (estimated by ICRP model) and relative abundance of the size-segregated PAHs in the head airway, tracheobronchial, and alveolar region of in the human respiratory tract.

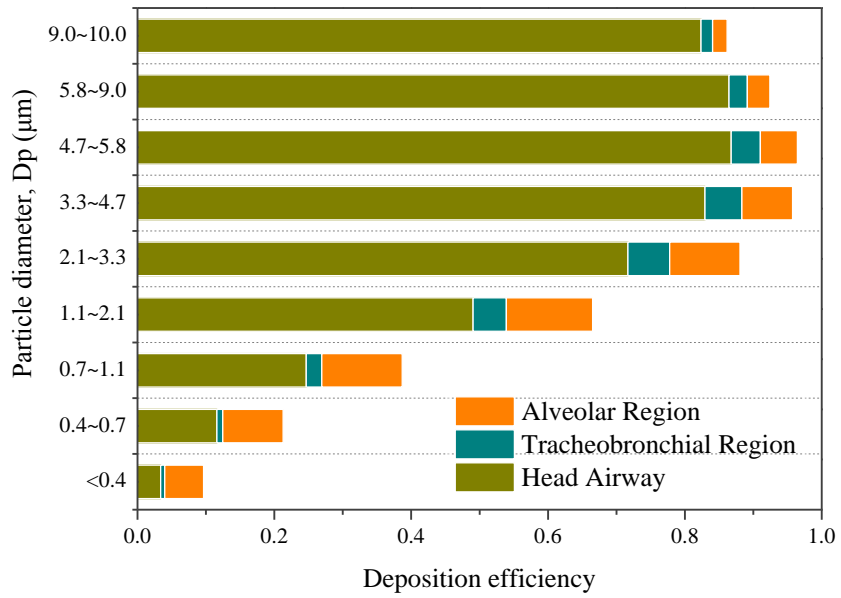
10

15

20

25





5

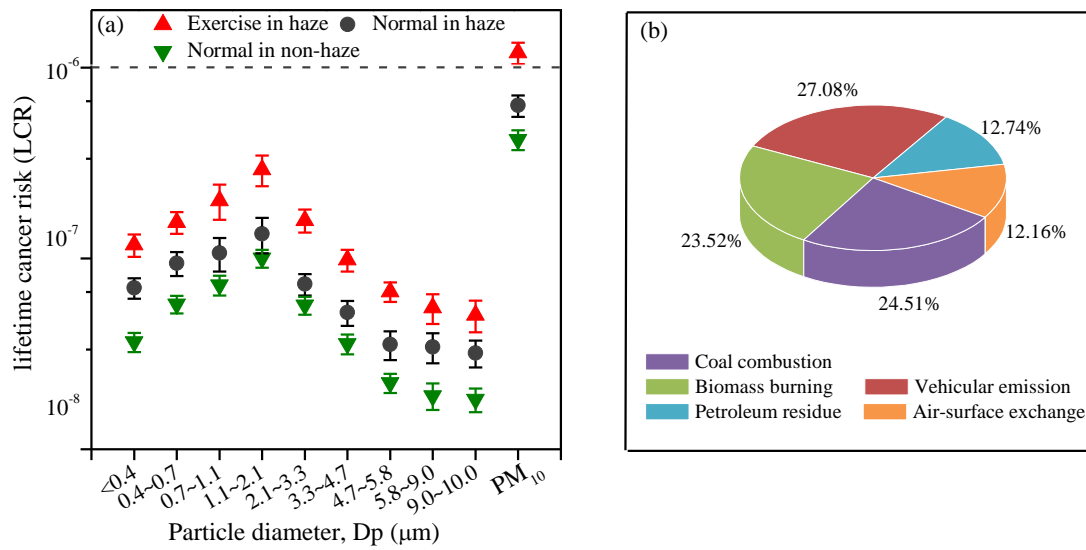
**Fig. 11.** Deposition efficiencies (estimated by ICRP model) of the size-segregated PAHs in the head airway, tracheobronchial, and alveolar region.

10

15

20

25



5 **Figure 13** **Fig. 12.** (a) Lifetime cancer risk (LCR) due to exposure to the size-segregated PAHs through inhalation for normal and exercise people during haze and non-haze period. (b) Source contribution to accumulation mode PAHs during haze period by PMF analysis.